

# Quantum Stochastic Walks for Portfolio Optimization: Theory and Implementation on Financial Networks

Yen Jui Chang<sup>1,2\*</sup>, Wei-Ting Wang<sup>3</sup>, Yun-Yuan Wang<sup>4</sup>,  
 Chen-Yu Liu<sup>5</sup>, Kuan-Cheng Chen<sup>6,7</sup>, Ching-Ray Chang<sup>2,3</sup>

<sup>1</sup>\*Master Program in Intelligent Computing and Big Data, Chung Yuan Christian University, No. 200, Zhongbei Rd., Zhongli Dist, Taoyuan City, 320314, Taiwan.

<sup>2</sup>Quantum Information Center, Chung Yuan Christian University, No. 200, Zhongbei Rd., Zhongli Dist, Taoyuan City, 320314, Taiwan.

<sup>3</sup>Department of Physics, National Taiwan University, No. 1, Sec. 4, Roosevelt Rd., Taipei, 106319, Taiwan.

<sup>4</sup>NVIDIA AI Technology Center, NVIDIA Corp., Taipei, Taiwan.

<sup>5</sup>Graduate Institute of Applied Physics, National Taiwan University, No. 1, Sec. 4, Roosevelt Rd., Taipei, 106319, Taiwan.

<sup>6</sup>Department of Electrical and Electronic Engineering, Imperial College London, London, UK.

<sup>7</sup>Centre for Quantum Engineering, Science and Technology (QuEST), Imperial College London, London, UK.

\*Corresponding author(s). E-mail(s): [aceest@cycu.edu.tw](mailto:aceest@cycu.edu.tw);  
 Contributing authors: [d11245002@ntu.edu.tw](mailto:d11245002@ntu.edu.tw); [yunyuanw@nvidia.com](mailto:yunyuanw@nvidia.com);  
[d10245003@g.ntu.edu.tw](mailto:d10245003@g.ntu.edu.tw); [kuan-cheng.chen17@imperial.ac.uk](mailto:kuan-cheng.chen17@imperial.ac.uk);  
[crchang@phys.ntu.edu.tw](mailto:crchang@phys.ntu.edu.tw);

## Abstract

Financial markets are noisy yet contain a latent graph-theoretic structure that can be exploited for superior risk-adjusted returns. We propose a *quantum-stochastic-walk* (QSW) optimizer that embeds assets in a weighted graph—nodes are securities, edges encode the return–covariance kernel—and derives portfolio weights from the stationary distribution of the walk. Three empirical studies support the method. (i) On the **Top-100 S&P constituents** (2016–2024)

six scenario portfolios fitted on 1- and 2-year windows lift the out-of-sample Sharpe ratio by up to **+27 %** while slashing annual turnover from **480%** (mean-variance) to **2–90%**. (ii) A **625** grid search isolates a robust sweet-spot— $\alpha, \lambda \lesssim 0.5, \omega \in [0.2, 0.4]$ —that delivers Sharpe  $\approx 0.97$  at  $\leq 5\%$  turnover and Herfindahl–Hirschman index(HHI)  $\sim 0.01$ . (iii) Repeating the full grid on **50 random 100-stock subsets** of the S&P 500 generates 31,350 additional back-tests: the best-per-draw QSW beats re-optimized mean–variance on Sharpe in 54 % of samples and *always* wins on trading efficiency, with median turnover **36 %** versus **351 %**. Overall, QSW raises the annualized Sharpe ratio by **15 %** and cuts average turnover by **90 %** relative to classical optimization, all while remaining comfortably within UCITS 5/10/40 rule. The findings demonstrate that hybrid quantum–classical dynamics can uncover non-linear dependencies overlooked by quadratic models, offering a practical low-cost weighting engine for themed ETFs and other systematic mandates.

**Keywords:** quantum finance, portfolio optimization, quantum stochastic walks, complex networks

## 1 Introduction

Modern investment management operates in an arena of high-dimensional, tightly coupled, and rapidly evolving data. Conventional quantitative techniques—most notably the seminal mean–variance framework of Markowitz [1]—encapsulate the trade-off between expected return and risk through a *quadratic* objective that minimizes portfolio variance for a target mean return. While mathematically elegant, this quadratic form becomes fragile when confronted with today’s realities: estimation error in large covariance matrices, non-Gaussian return distributions, time-varying correlations, and a proliferation of real-world constraints such as turnover limits, liquidity frictions, and regulatory capital charges [2–6].

### *From quadratic programming to graph dynamics.*

Early econophysics research showed that a covariance matrix can be *filtered* into a sparse network via minimum-spanning trees or planar maximally filtered graphs whose topology reflects hidden economic sectors and contagion channels [7–9]. Subsequent work demonstrated that risk propagation and systemic fragility travel along these edges much like a diffusion process [10, 11]. We therefore reinterpret the Markowitz objective as assigning a probability measure over such a graph: edge flows penalize high covariance, while self-loops reward each asset’s risk-adjusted return. Capturing this diffusion explicitly motivates the textbf{dual-channel} approach pursued in this work.

### *Quantum stochastic walks as a dual-channel engine*

Recent progress in quantum information science—including decoherence-controlled *quantum stochastic walks* (QSWs) [12, 13]—and quantum network-ranking algorithms [14–17] makes it possible to merge coherent quantum evolution with classical

random walks on the same graph. The **coherent channel**, governed by a Hermitian Hamiltonian, explores the network through superposition and interference, while a **stochastic channel** guarantees ergodicity and convergence. By tuning the quantum-classical mixing parameter, QSWs interpolate smoothly between fully quantum exploration and purely classical diffusion, providing an adaptive mechanism well suited to financial systems that exhibit both structured dependencies and stochastic shocks.

### *Contributions of this work*

Building on these insights, we develop a *quantum graph-theoretic* framework for portfolio optimization that

- (i) maps mean returns, volatilities, and covariances to a weighted, directed graph whose self-loops retain the asset-specific Sharpe ratio and whose inter-node edges penalize correlation;
- (ii) deploys a dual-channel QSW to evolve a density matrix whose diagonal converges to steady-state asset weights, thereby realizing the quadratic mean-risk balance *via* graph dynamics;
- (iii) implements the algorithm on GPU hardware, enabling real-time optimization over universes of 100 assets; and
- (iv) empirically benchmarks the resulting portfolios against maximum-Sharpe mean-variance solutions and the capitalization-weighted S&P 500 index.

Comprehensive back-testing demonstrates that incorporating quantum coherence yields higher Sharpe ratios and lower turnover than classical optimization without sacrificing diversification. Moreover, a large-scale grid search across 625 parameter combinations and 50 randomly selected sub-universes establishes the robustness of these gains.

This paper builds understanding systematically from classical foundations to quantum innovations. Section 2 identifies the five fundamental limitations of mean-variance optimization that motivate our quantum approach, providing the conceptual anchor readers need to appreciate why quantum methods offer genuine advantages. Section 3 bridges classical and quantum domains by showing how financial networks naturally support QSW dynamics. Section 4 translates theory into practice through GPU-accelerated algorithms and comprehensive experimental design. Section 5 demonstrates that quantum-enhanced portfolios consistently outperform classical alternatives across multiple metrics and market conditions. Section 6 synthesizes the findings and explores practical implementation pathways for quantum portfolio management.

## 2 Classical Portfolio Optimization: Foundations and Limitations

The classical approach to portfolio optimization has served as the bedrock of quantitative finance for over seven decades. In this section, we review the fundamental principles underlying traditional portfolio theory and critically examine its limitations

in addressing the complexities of modern financial markets. This analysis provides the necessary context for understanding how quantum methods can transcend these classical boundaries.

## 2.1 Mean-Variance Framework

The seminal work of Harry Markowitz [1] established the mean-variance optimization framework, which remains the cornerstone of modern portfolio theory. This framework elegantly balances the trade-off between expected returns and risk, measured as variance of returns. The theoretical foundations were further developed by Tobin [18], who introduced the separation theorem, Sharpe [19], who developed the Capital Asset Pricing Model (CAPM), and Merton [20], who provided analytical solutions for dynamic portfolio problems.

Consider a universe of  $n$  risky assets with random returns  $\mathbf{r} = (r_1, r_2, \dots, r_n)^T$ . The expected return vector is denoted as  $\boldsymbol{\mu} = \mathbb{E}[\mathbf{r}] = (\mu_1, \mu_2, \dots, \mu_n)^T$ , and the covariance matrix is  $\boldsymbol{\Sigma} = \text{Cov}(\mathbf{r}) \in \mathbb{R}^{n \times n}$ , where element  $\Sigma_{ij} = \text{Cov}(r_i, r_j)$ .

For a portfolio with weight vector  $\mathbf{w} = (w_1, w_2, \dots, w_n)^T$ , where  $w_i$  represents the fraction of wealth invested in asset  $i$ , the portfolio return is:

$$r_p = \mathbf{w}^T \mathbf{r} = \sum_{i=1}^n w_i r_i \quad (1)$$

The expected portfolio return and variance are given by:

$$\mu_p = \mathbb{E}[r_p] = \mathbf{w}^T \boldsymbol{\mu} \quad (2)$$

$$\sigma_p^2 = \text{Var}(r_p) = \mathbf{w}^T \boldsymbol{\Sigma} \mathbf{w} \quad (3)$$

The classical mean-variance optimization problem can be formulated in multiple equivalent forms:

**Minimum Variance Problem:**

$$\begin{aligned} \min_{\mathbf{w}} \quad & \frac{1}{2} \mathbf{w}^T \boldsymbol{\Sigma} \mathbf{w} \\ \text{subject to} \quad & \mathbf{w}^T \boldsymbol{\mu} \geq \mu_{\text{target}} \\ & \mathbf{w}^T \mathbf{1} = 1 \\ & \mathbf{w} \geq \mathbf{0} \end{aligned} \quad (4)$$

where  $\mu_{\text{target}}$  is the desired minimum expected return,  $\mathbf{1}$  is a vector of ones, and the inequality  $\mathbf{w} \geq \mathbf{0}$  enforces no short-selling constraints.

**Maximum Sharpe Ratio Problem:**

$$\begin{aligned} \max_{\mathbf{w}} \quad & \frac{\mathbf{w}^T \boldsymbol{\mu} - r_f}{\sqrt{\mathbf{w}^T \boldsymbol{\Sigma} \mathbf{w}}} \\ \text{subject to} \quad & \mathbf{w}^T \mathbf{1} = 1 \\ & \mathbf{w} \geq \mathbf{0} \end{aligned} \quad (5)$$

where  $r_f$  denotes the risk-free rate.

The solution to the unconstrained problem yields the efficient frontier, characterized by:

$$\mathbf{w}^* = \frac{\boldsymbol{\Sigma}^{-1}(\boldsymbol{\mu} - \lambda \mathbf{1})}{\mathbf{1}^T \boldsymbol{\Sigma}^{-1}(\boldsymbol{\mu} - \lambda \mathbf{1})} \quad (6)$$

where  $\lambda$  is a Lagrange multiplier that parameterizes different points along the efficient frontier.

## 2.2 Extensions and Refinements

Several extensions to the basic mean-variance framework have been proposed to address specific practical considerations:

**Black-Litterman Model:** Black and Litterman [3] developed a Bayesian approach that combines market equilibrium with investor views:

$$\boldsymbol{\mu}_{BL} = [(\tau \boldsymbol{\Sigma})^{-1} + \mathbf{P}^T \boldsymbol{\Omega}^{-1} \mathbf{P}]^{-1} [(\tau \boldsymbol{\Sigma})^{-1} \boldsymbol{\Pi} + \mathbf{P}^T \boldsymbol{\Omega}^{-1} \mathbf{q}] \quad (7)$$

where  $\boldsymbol{\Pi}$  represents equilibrium returns,  $\mathbf{P}$  encodes views,  $\mathbf{q}$  represents view magnitudes,  $\boldsymbol{\Omega}$  is the uncertainty in views, and  $\tau$  is a scaling parameter.

**Robust Optimization:** To address parameter uncertainty, robust formulations have been developed [2, 21, 22]:

$$\begin{aligned} & \min_{\mathbf{w}} \max_{\boldsymbol{\mu} \in \mathcal{U}_\mu, \boldsymbol{\Sigma} \in \mathcal{U}_\Sigma} \mathbf{w}^T \boldsymbol{\Sigma} \mathbf{w} \\ & \text{subject to } \mathbf{w}^T \boldsymbol{\mu} \geq \mu_{\text{target}} \\ & \mathbf{w}^T \mathbf{1} = 1 \end{aligned} \quad (8)$$

where  $\mathcal{U}_\mu$  and  $\mathcal{U}_\Sigma$  represent uncertainty sets for parameters.

**Resampled Efficiency:** Michaud [23] introduced resampling techniques to address estimation error, while coherent risk measures [24] and conditional value-at-risk (CVaR) optimization [25] provide alternatives to variance as a risk metric.

## 2.3 Limitations

Despite its theoretical elegance and widespread adoption, the classical mean-variance framework faces numerous limitations when applied to real-world investment problems:

### *Curse of Dimensionality and Estimation Error*

The covariance matrix  $\boldsymbol{\Sigma}$  contains  $\frac{n(n+1)}{2}$  unique parameters that must be estimated from historical data. For a modest universe of  $n = 500$  assets, this requires estimating 125,250 parameters. Given finite sample sizes, estimation errors compound dramatically, leading to unstable and suboptimal portfolios [4]. Indeed, DeMiguel et al. [26] demonstrated that a naive  $1/n$  equal-weighted portfolio often outperforms sophisticated optimization techniques out-of-sample, highlighting the severity of estimation error.

The condition number of the covariance matrix, defined as:

$$\kappa(\Sigma) = \frac{\lambda_{\max}(\Sigma)}{\lambda_{\min}(\Sigma)} \quad (9)$$

often exceeds  $10^6$  for large asset universes, indicating severe ill-conditioning that amplifies small estimation errors into large portfolio weight distortions.

### ***Non-Stationarity and Regime Changes***

Financial markets exhibit time-varying statistical properties, violating the stationarity assumption underlying classical optimization. The dynamic nature of correlations can be characterized by:

$$\rho_{ij,t} = \frac{\text{Cov}_t(r_i, r_j)}{\sigma_{i,t}\sigma_{j,t}} \quad (10)$$

where subscript  $t$  denotes time-dependence. During market crises, correlations often converge toward unity, precisely when diversification is most needed [7]. Longin and Solnik [27] documented that correlations increase significantly during market downturns, while Ang and Chen [28] revealed asymmetric correlations between upside and downside movements.

### ***Non-Gaussian Return Distributions***

Empirical asset returns exhibit significant departures from normality, including:

- **Heavy tails:** Excess kurtosis  $\kappa = \mathbb{E}[(r - \mu)^4]/\sigma^4 - 3 > 0$
- **Asymmetry:** Non-zero skewness  $\gamma = \mathbb{E}[(r - \mu)^3]/\sigma^3$
- **Volatility clustering:** Time-varying conditional variance

Cont [29] provides a comprehensive review of these stylized facts, showing that return distributions exhibit power-law tails with tail indices typically between 2 and 5. These features render variance an inadequate risk measure, as it fails to capture tail risks and higher-order moments that significantly impact portfolio performance.

### ***Computational Complexity with Realistic Constraints***

Practical portfolio optimization often involves constraints beyond the simple linear constraints in Equation (4):

#### **Cardinality Constraints:**

$$\sum_{i=1}^n \mathbb{I}(w_i > 0) \leq K \quad (11)$$

where  $\mathbb{I}(\cdot)$  is the indicator function and  $K$  limits the number of holdings. Chang et al. [30] and Bienstock [31] demonstrated that portfolio optimization with cardinality constraints is NP-hard.

### Transaction Costs:

$$TC = \sum_{i=1}^n c_i |w_i - w_{i,0}| \quad (12)$$

where  $c_i$  represents the transaction cost rate and  $w_{i,0}$  is the initial weight.

### Market Impact:

$$\text{Impact}_i = \alpha_i \cdot \text{sgn}(w_i - w_{i,0}) \cdot |w_i - w_{i,0}|^{\beta_i} \quad (13)$$

Almgren and Chriss [32] developed optimal execution strategies that account for both permanent and temporary market impact, while Grinold and Kahn [33] integrated transaction costs into the portfolio construction process.

The inclusion of such constraints transforms the problem from a convex quadratic program to a mixed-integer nonlinear program (MINLP), which is NP-hard [6].

### Sensitivity to Input Parameters

Small perturbations in expected returns can lead to dramatic changes in optimal portfolios. Best and Grauer [34] showed that mean-variance portfolios are extremely sensitive to estimates of expected returns, while Chopra and Ziemba [35] quantified that errors in means are roughly eleven times as important as errors in variances, and errors in variances are twice as important as errors in covariances. The sensitivity can be quantified by:

$$\frac{\partial \mathbf{w}^*}{\partial \boldsymbol{\mu}} = \frac{1}{\mathbf{1}^T \boldsymbol{\Sigma}^{-1} \mathbf{1}} \left[ \boldsymbol{\Sigma}^{-1} - \frac{\boldsymbol{\Sigma}^{-1} \mathbf{1} \mathbf{1}^T \boldsymbol{\Sigma}^{-1}}{\mathbf{1}^T \boldsymbol{\Sigma}^{-1} \mathbf{1}} \right] \quad (14)$$

This extreme sensitivity often results in concentrated, unintuitive portfolios that perform poorly out of sample.

### Failure to Capture Complex Dependencies

Classical correlation measures only capture linear dependencies:

$$\rho_{ij} = \frac{\text{Cov}(r_i, r_j)}{\sigma_i \sigma_j} \quad (15)$$

However, financial markets exhibit complex nonlinear dependencies, tail dependencies, and higher-order interactions that are invisible to linear correlation analysis. Copula-based measures reveal that:

$$\tau_{\text{tail}} = \lim_{u \rightarrow 1} P(F_j(r_j) > u | F_i(r_i) > u) \quad (16)$$

often differs significantly from what linear correlation would predict.

## 2.4 Practical Limitations of Classical Optimization

Despite seven decades of refinement, mean-variance optimization faces fundamental challenges when applied to real-world portfolio construction:

- (a) **Estimation error and dimensionality.** The covariance matrix  $\Sigma$  contains  $\frac{1}{2}n(n + 1)$  parameters; with  $n = 500$  assets this exceeds  $1.25 \times 10^5$  parameters. Finite samples routinely yield condition numbers  $\kappa(\Sigma) > 10^6$ , causing extreme sensitivity to estimation errors and unstable portfolio weights [26].
- (b) **Market non-stationarity.** Correlations spike toward unity during market crises [27], precisely when diversification is most crucial. This violates the stationarity assumption underlying Equation (4) and renders historical covariance estimates unreliable for forward-looking optimization.
- (c) **Non-Gaussian return distributions.** Empirical returns exhibit heavy tails, asymmetric skewness, and volatility clustering [29]. Variance captures only second-moment risk, ignoring tail dependencies and higher-order interactions that dominate crisis periods.
- (d) **Real-world implementation constraints.** Practical considerations—cardinality limits, transaction costs, market impact, and liquidity constraints—transform the convex quadratic program into an NP-hard mixed-integer nonlinear program [6, 30], often requiring heuristic approximations.
- (e) **Extreme parameter sensitivity.** Small perturbations in expected returns  $\mu$  cause dramatic portfolio rebalancing. Estimation errors in means dominate those in covariances by roughly an order of magnitude [34, 35], leading to unstable and counterintuitive allocations.

## 2.5 Why a Quantum–Graph Perspective?

The classical mean–variance framework treats portfolio choice as a *static* quadratic programme, yet the risk term  $\mathbf{w}^\top \Sigma \mathbf{w}$  can be viewed more intuitively as a **diffusion of capital** on a weighted network: assets form the vertices, covariances set the edge weights, and self-loops reward each asset’s own risk-adjusted return. Network studies based on minimum-spanning trees (MST) and planar maximally filtered graphs (PMFG) first revealed that diversification and contagion propagate along these edges [7–9]. Later work traced systemic-risk spill-overs across such graphs [10, 11]. Classical solvers glimpse this structure only indirectly through dense linear algebra, which neither adapts on-line to time-varying edges nor embeds diversification *in the dynamics* of the flow.

### *Quantum Stochastic Walks (QSWs) as a dual-channel engine.*

A QSW blends coherent quantum evolution with a stochastic Google-type walk [12–15]. The coherent channel, driven by a Hamiltonian, explores correlated asset clusters through superposition and interference; the stochastic channel, parameterized by the Google matrix [36], guarantees ergodicity and convergence. Tuning the quantum-classical mixing parameter  $\omega$  turns this into an adaptive mechanism ideally suited to markets that exhibit both structured dependencies and stochastic shocks.

- **Correlated clusters explored coherently.** Superposition surveys multiple highly-covariant groups in parallel, uncovering hidden diversification routes.
- **Diversification via decoherence.** The stochastic channel damps cyclic probability within tight clusters, nudging capital towards under-represented sectors.

- **Non-linear dependencies captured.** Interference patterns encode higher-order effects that linear correlation omits.
- **Guaranteed convergence.** For any  $\omega > 0$ , the GKLS generator with Google matrix formulation is relaxing; the walk converges exponentially fast to a unique stationary state [37].
- **Scalable like PageRank.** Sparse matrix–vector kernels identical to web ranking allow GPU or distributed implementations on universes of  $10^3\text{--}10^4$  assets.

Thus the quantum–graph view transforms portfolio optimization from a brittle quadratic fit into a living, ergodic process that balances exploration and exploitation on the financial network itself. Sections 3–4 formalize this construction and show how it subsumes Eqs. (4)–(5), addressing the five classical limitations identified in Section 2.4 while delivering empirically superior risk-adjusted returns.

### 3 Quantum Stochastic Walks: From Theory to Financial Formulation

QSWs extend classical random walks by blending coherent quantum evolution with controlled decoherence. This dual-channel design overcomes the shortcomings of purely classical diffusion, no higher-order interference, and purely quantum walks, no stationary state, making QSWs a natural engine for portfolio allocation on financial graphs.

#### 3.1 Mathematical foundations

##### *Random walks and PageRank.*

Classical random walks on graphs have long served as fundamental models in network analysis. For a graph  $G = (V, E)$  with  $n$  nodes representing financial assets, a continuous-time random walk is governed by the master equation:

$$\frac{d\vec{p}}{dt} = (P - I)\vec{p} \quad (17)$$

where  $\vec{p} = (p_1, p_2, \dots, p_n)^T$  represents the probability distribution over nodes and  $P$  is the transition matrix.

The PageRank algorithm [36] enhances this framework by introducing teleportation:

$$\mathcal{G} = \alpha_{\text{damp}} P + (1 - \alpha_{\text{damp}}) \frac{\mathbf{1}\mathbf{1}^T}{n} \quad (18)$$

where  $\alpha_{\text{damp}} \in (0, 1)$  is the damping parameter (typically 0.9) and  $\mathbf{1}\mathbf{1}^T$  is the  $n \times n$  all-ones matrix. This construction ensures ergodicity and unique stationary distribution even for directed graphs with dangling nodes.

##### *Continuous-time quantum walks.*

Continuous-time quantum walks (CTQWs) replace the classical probability distribution  $\vec{p}$  with a quantum state  $|\psi\rangle$  evolving under the Schrödinger equation

[38, 39]:

$$i\hbar \frac{d|\psi\rangle}{dt} = H|\psi\rangle \quad (19)$$

The quantum state evolves as  $|\psi(t)\rangle = e^{-iHt/\hbar}|\psi(0)\rangle$ , and the probability of finding the walker at node  $j$  is  $P_j(t) = |\langle j|\psi(t)\rangle|^2$ . While CTQWs can achieve quadratic speedups for certain graph problems [40], they lack a stationary state and are highly sensitive to decoherence.

### Quantum Stochastic Walks

QSWs interpolate between Eqs. (17) and (19) via the Gorini–Kossakowski–Lindblad–Sudarshan (GKLS) master equation [17]:

$$\frac{d\rho}{dt} = -i(1-\omega)[H, \rho] + \omega \sum_{i,j} c_{ij} \left( L_{ij}\rho L_{ij}^\dagger - \frac{1}{2}\{L_{ij}^\dagger L_{ij}, \rho\} \right), \quad (20)$$

where:

- $\rho$  is the density matrix describing the quantum state
- $\omega \in [0, 1]$  is the mixing parameter controlling the quantum-classical balance
- $H$  is the Hamiltonian governing coherent evolution
- $L_{ij} = |i\rangle\langle j|$  are Lindblad jump operators
- $c_{ij} \geq 0$  are transition rates

The GKLS master equation (20) describes **QSWs** in open quantum systems, providing a unified framework that smoothly interpolates between purely classical random walks and coherent quantum walks.

The equation consists of **two competing terms**:

1. **Coherent Evolution:** The commutator term  $-i(1-\omega)[H, \rho]$  drives unitary quantum dynamics, preserving quantum coherence and enabling quantum interference effects characteristic of pure quantum walks.
2. **Dissipative Dynamics:** The Lindblad term  $\omega \sum_{i,j} c_{ij}(\cdot)$  introduces environmental decoherence and classical jump processes, causing the system to behave more like a classical random walk.

The **mixing parameter**  $\omega \in [0, 1]$  controls the quantum-classical balance:

- $\omega = 0$ : Pure coherent quantum walk (Schrödinger evolution)
- $\omega = 1$ : Classical stochastic process
- $0 < \omega < 1$ : Hybrid quantum-classical dynamics

A fundamental requirement for optimization applications is convergence to a unique stationary state.

**Theorem 1** (Stationary state of a QSW) *Let  $c_{ij} = \mathcal{G}_{ij}$  where  $\mathcal{G}$  is the Google matrix (18). For any  $\omega > 0$  the quantum dynamical semigroup generated by Eq. (20) is primitive: a unique, full-rank stationary state  $\rho_\infty$  exists and  $\rho(t) \rightarrow \rho_\infty$  exponentially fast [37]. We set final asset weights  $w_i = \rho_{\infty,ii}$ .*

### 3.2 Encoding financial data on a graph

#### *Node Representation*

Given  $n$  financial assets with historical returns, each node  $i \in \{1, 2, \dots, n\}$  is characterized by mean return  $\mu_i$ , volatility  $\sigma_i$ , and daily Sharpe ratio  $SR_i = \mu_i/\sigma_i$ .

#### *Weight Matrix Construction*

The graph weight matrix  $W$  encodes both individual asset quality and pairwise relationships through an exponential transformation:

$$W_{ij} = \begin{cases} \exp(\alpha SR_j - \beta \Sigma_{ij}) & \text{if } i \neq j \\ \exp(\lambda SR_i) & \text{if } i = j \end{cases} \quad (21)$$

where:

- $\alpha > 0$  controls the preference for high-Sharpe-ratio destinations
- $\beta > 0$  penalizes transitions between correlated assets
- $\Sigma_{ij}$  is the covariance between assets  $i$  and  $j$
- $\lambda$  is the holding coefficient for self-loops

This formulation creates a preference landscape where:

1. Transitions to high-Sharpe assets are favored (through  $\alpha SR_j$ )
2. Transitions between highly correlated assets are penalized (through  $-\beta \Sigma_{ij}$ )
3. Holding positions in high-Sharpe assets is rewarded (diagonal terms)

Figure 1 translates the eight-stock toy universe into the fully-connected graph governed by Eq. (21). Nodes carry each asset's ticker and one-day Sharpe ratio; directed edges depict the off-diagonal weights  $W_{ij}$ . Together, width and color make the opposing forces of  $\alpha$  (*Sharpe attraction*) and  $\beta$  (*covariance repulsion*) visually obvious: high-Sharpe, low-covariance pairs shine as thick yellow edges, whereas transitions between noisy or tightly co-moving stocks recede into the background.

### 3.3 Dual-Channel Quantum Encoding

Our framework encodes financial information through two complementary channels that capture different aspects of market dynamics.

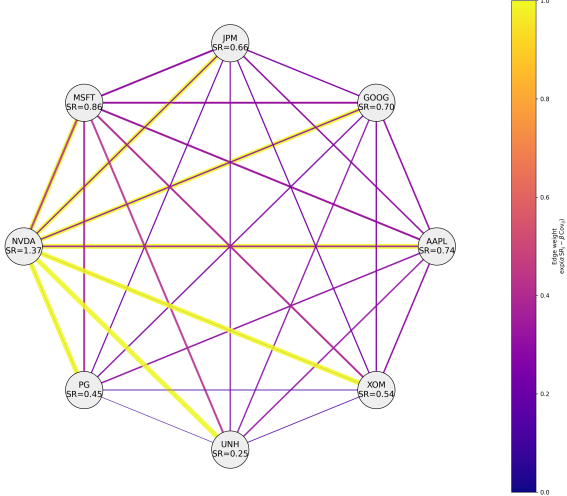


**Fig. 1:** Encoding an eight-stock toy universe as a fully-connected graph. Node size is proportional to the asset's one-day Sharpe ratio, and each directed edge ( $i \rightarrow j$ ) is drawn with width  $\propto W_{ij}$  and color given by a PLASMA scale of the same weight (see Eq. (21)). Thick yellow edges therefore highlight moves favored by high Sharpe and low covariance, while thin purple edges indicate transitions suppressed by the covariance penalty  $\beta$ .

#### Coherent Channel: Hamiltonian Construction

**Coherent channel** explores highly correlated clusters via quantum tunneling and interference. The Hamiltonian governs the quantum coherent evolution and encodes both individual asset quality and correlation structure:

$$H_{ij} = \begin{cases} -\gamma_1 \cdot SR_i & \text{if } i = j \\ \gamma_2 \cdot \hat{\Sigma}_{ij} & \text{if } i \neq j \end{cases} \quad (22)$$

where  $\gamma_1 = \gamma_2 = 100$  are scaling factors and  $\hat{\Sigma}_{ij}$  is the normalized covariance:

$$\hat{\Sigma}_{ij} = \frac{\Sigma_{ij} - \Sigma_{\min}}{\Sigma_{\max} - \Sigma_{\min}} \quad (23)$$

This normalization ensures  $\hat{\Sigma}_{ij} \in [0, 1]$  and provides numerical stability. The scaling factor of 100 ensures the Hamiltonian elements have appropriate magnitude for numerical evolution.

The Hamiltonian design achieves several objectives:

1. **Energy landscape:** Diagonal terms create an energy gradient favoring high-Sharpe assets (lower energy)

2. **Quantum tunneling:** Off-diagonal terms enable coherent transitions based on the covariance structure
3. **Hermiticity:** The construction ensures  $H_{ij} = H_{ji}$ , preserving unitarity

#### *Stochastic Channel: Google Matrix Rates*

**Stochastic channel** enforces diversification through teleportation and correlation-weighted penalties. The weight matrix is row-normalized to create a stochastic transition matrix:

$$P_{ij} = \frac{W_{ij}}{\sum_k W_{ik}} \quad (24)$$

Then implemented in the Google matrix(18)

The stochastic dynamics are implemented through transition rates in Eq. (20) derived from the Google matrix:

$$c_{ij} = \mathcal{G}_{ij} \quad (25)$$

When set proportional to Google matrix elements, the rates  $c_{ij}$  intuitively represent:

- **Capital flow propensity:** Risk- and return-weighted tendency to reallocate from asset  $j$  to asset  $i$
- **Liquidity constraints:** Small  $c_{ij}$  for illiquid or high-friction transitions
- **Market microstructure:** Can be calibrated to empirical trade flow intensities

The QSW framework provides several quantum advantages over classical approaches:

#### *Simultaneous Exploration of Portfolio Space*

The quantum superposition enables exploration of multiple portfolio configurations simultaneously. Starting from the maximally mixed state:

$$\rho_0 = \frac{I}{n} \quad (26)$$

the system evolves through a superposition of paths weighted by both:

- Quantum amplitudes (from Hamiltonian evolution)
- Classical probabilities (from Google matrix transitions)

This dual exploration mechanism can discover portfolio allocations that satisfy multiple criteria simultaneously.

#### *Correlation-Aware Portfolio Construction*

The interplay between the two channels creates sophisticated portfolio dynamics:

1. **Hamiltonian channel:** The normalized covariance in off-diagonal terms enables quantum tunneling between correlated assets, allowing the system to explore correlation clusters coherently

2. **Google channel:** The exponential penalty  $\exp(-\beta\Sigma_{ij})$  in transition rates suppresses classical jumps between correlated assets, encouraging diversification

This dual treatment of correlations—quantum tunneling within clusters but classical suppression between them—naturally identifies diversified portfolios.

#### ***Adaptive Risk-Return Balance***

The QSW framework provides control over optimization behavior through multiple parameters:

##### ***Mixing Parameter $\omega$***

Controls the quantum-classical balance:

- Low  $\omega$  (e.g., 0.2): Quantum effects dominate, enabling broad exploration
- High  $\omega$  (e.g., 0.8-1.0): Classical dynamics dominate, ensuring convergence
- Medium  $\omega$  (e.g., 0.4-0.6): Balanced regime for most market conditions

##### ***Return Preference $\alpha$***

Controls the strength of preference for high-Sharpe assets in the weight matrix:

- Low  $\alpha$  (e.g., 0.1): Weak preference, allowing broader asset selection
- High  $\alpha$  (e.g., 100-500): Strong preference for high-Sharpe assets
- Affects the exponential weight  $W_{ij} \propto \exp(\alpha SR_j)$

##### ***Diversification Strength $\beta$***

Controls the penalty for correlated assets:

- Low  $\beta$  (e.g., 0.1): Weak correlation penalty, allowing concentrated portfolios
- High  $\beta$  (e.g., 100-500): Strong penalty, enforcing diversification
- Affects the exponential weight  $W_{ij} \propto \exp(-\beta\Sigma_{ij})$

##### ***Holding Coefficient $\lambda$***

Controls the incentive to maintain positions:

- Low  $\lambda$  (e.g., 0.1): Weak holding incentive, allowing frequent rebalancing
- High  $\lambda$  (e.g., 100-500): Strong incentive to maintain current positions
- Affects diagonal weights  $W_{ii} = \exp(\lambda SR_i)$

These parameters offer flexibility in tailoring the optimization to different investment objectives and market conditions. The optimal parameter values depend on the specific application and can be determined through a systematic grid search or optimization.

### 3.4 Summary and outlook

This section establishes the theoretical foundations of QSWs and their application to financial scenarios. We have shown how QSWs bridge quantum and classical dynamics through controlled decoherence, enabling both quantum exploration advantages and guaranteed convergence to stable portfolio weights.

Key theoretical contributions include:

1. Mathematical framework combining coherent quantum evolution with classical stochastic processes
2. Proof of convergence to unique stationary states under mild conditions
3. Financial interpretation of quantum parameters in terms of market dynamics
4. Demonstration of theoretical advantages over classical optimization methods

The framework offers significant flexibility through its multiple parameters ( $\omega, \alpha, \beta, \lambda$ ), which can be optimized for different market conditions and investment objectives. While our current implementation uses fixed parameters determined through grid search, future work could explore adaptive parameter schemes that respond dynamically to market indicators such as volatility (VIX), correlation levels, and liquidity conditions.

These theoretical foundations provide the basis for practical implementation. In the following section, we present the computational methodology for implementing QSWs efficiently, along with comprehensive evaluation metrics to demonstrate their effectiveness in real-world portfolio optimization.

## 4 Implementation and Evaluation Methodology

Building on the theoretical framework and financial formulation presented in Section 3, this section details the practical implementation of the QSWs portfolio optimization algorithm and the comprehensive experimental framework used to validate its effectiveness against classical benchmarks.

Building directly on the quantum-stochastic formalism of Section 3, Figure 2 distils the *end-to-end implementation pipeline* into four sequential stages:

**Stage 1: Data processing** – ingest daily close prices, transform them into log-returns, and compute the sample covariance matrix  $S$ .

**Stage 2: Two-channel graph** – embed the data in a dual network:

- *Stochastic channel*: Google matrix  $G_{ij} \propto \exp(\alpha \text{SR}_j - \beta \Sigma_{ij})$  that favours moves toward high-Sharpe, low-covariance destinations.
- *Coherent channel*: Hamiltonian  $H_{ii} \propto \text{SR}_i, H_{ij} \propto \Sigma_{ij}$  ( $i \neq j$ ), capturing quantum interference effects.

**Stage 3: QSW solver** – iterate the density operator under the quantum-classical mix  $\omega$  until convergence to the stationary distribution  $p^*$ .

**Stage 4: Weights** – convert  $p^*$  into fully-invested portfolio weights,  $\sum_i w_i = 1$ , which are then fed into the back-test loop or an ETF wrapper.

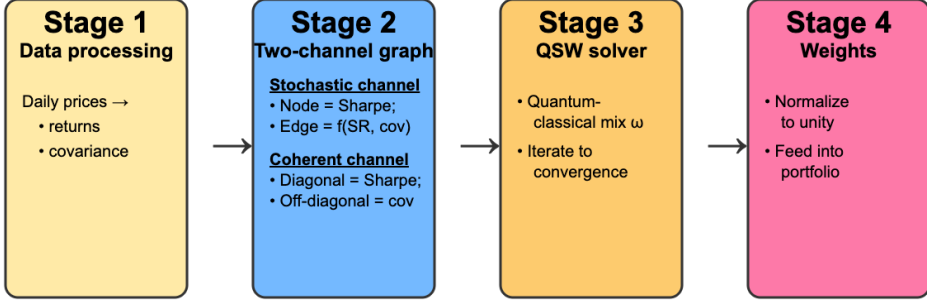


**Fig. 2:** Four-stage quantum-stochastic-walk (QSW) portfolio framework employed in all subsequent experiments.

#### 4.1 Quantum Stochastic Walks Algorithm Implementation

##### *Efficient Kraus Operator Implementation*

We implement the QSW evolution using the efficient Kraus operator formulation derived in Section 3. Traditionally, Eq. 20 is solved using the unraveling method of the master equation. However, this approach increases the matrix size from  $N$  to  $N^2$ , which leads to significant computational overhead. To accelerate the simulation, we map the Hamiltonian and Lindbladian operators  $\{H, L_{i,j}\}$  to a set of Kraus operators  $\{K_0, K_{i,j}\}$ , and implement the quantum channel using the operator-sum representation:

$$\rho(t+1) = K_0\rho(t)K_0^\dagger + \sum_{i,j} K_{i,j}\rho(t)K_{i,j}^\dagger, \quad (27)$$

where the Kraus operators satisfy the trace-preserving condition:

$$K_0^\dagger K_0 + \sum_{i,j} K_{i,j}^\dagger K_{i,j} = I. \quad (28)$$

The relation between the Lindblad equation and the Kraus operators can be derived by discretizing Eq. (4). This yields:

$$\begin{aligned}
\rho(t + \Delta t) &= \rho(t) - i\omega[H, \rho(t)]\Delta t \\
&\quad + \omega \sum_{i,j} c_{ij} \left( L_{i,j}\rho(t)L_{i,j}^\dagger - \frac{1}{2}\{L_{i,j}^\dagger L_{i,j}, \rho(t)\} \right) \Delta t \\
&= \left( I - i\omega H \Delta t - \frac{1}{2}\omega \sum_{i,j} c_{ij} L_{i,j}^\dagger L_{i,j} \Delta t \right) \rho(t) \\
&\quad \times \left( I + i\omega H \Delta t - \frac{1}{2}\omega \sum_{i,j} c_{ij} L_{i,j}^\dagger L_{i,j} \Delta t \right)
\end{aligned}$$

$$+ \omega \sum_{i,j} c_{ij} L_{i,j} \rho(t) L_{i,j}^\dagger \Delta t + \mathcal{O}(\Delta t^2). \quad (29)$$

By comparing Eq. (29) with Eq. (27), we approximate the Kraus operators as:

$$K_{i,j} = \sqrt{1 - e^{-\omega c_{ij} \Delta t}} L_{i,j}, \quad (30)$$

and

$$K_0 = \sqrt{I - \sum_{i,j} K_{i,j}^\dagger K_{i,j}} \cdot e^{-i(1-\omega)H\Delta t}. \quad (31)$$

In addition, the form of the Kraus operator in our case is  $\gamma_{ij}|i\rangle\langle j|$ , which is a very sparse matrix. Therefore, each matrix multiplication in the second term can be rewritten as

$$K_{i,j} \rho K_{i,j}^\dagger = (\gamma_{ij}|i\rangle\langle j|) \rho (\gamma_{ij}|j\rangle\langle i|) = \gamma_{ij}^2 \rho_{jj} |i\rangle\langle i|. \quad (32)$$

This shows that the second term in Eq. (27) only involves the diagonal elements of the density matrix. Hence, we can write

$$\sum_{i,j} K_{i,j} \rho K_{i,j}^\dagger = \Gamma P, \quad (33)$$

where

$$P = \begin{pmatrix} \rho_{11} \\ \rho_{22} \\ \vdots \\ \rho_{NN} \end{pmatrix}, \quad (34)$$

and

$$\Gamma = \begin{pmatrix} \gamma_{11}^2 & \gamma_{12}^2 & \cdots & \gamma_{1N}^2 \\ \gamma_{21}^2 & \gamma_{22}^2 & \cdots & \gamma_{2N}^2 \\ \vdots & \vdots & \ddots & \vdots \\ \gamma_{N1}^2 & \gamma_{N2}^2 & \cdots & \gamma_{NN}^2 \end{pmatrix}. \quad (35)$$

As a result, the summation of matrix multiplications in Eq. (27) is reduced to a single matrix-vector multiplication, and the operator-sum representation can be simplified as

$$\rho' = K_0 \rho K_0^\dagger + \Gamma P. \quad (36)$$

Therefore, the procedure for the proposed *Quantum PageRank-Based Portfolio Optimization* algorithm is outlined as follows:

---

**Algorithm 1** GPU-Accelerated Quantum PageRank for Portfolio Optimization

---

**Require:** Historical returns, QSW parameters  $\{\omega, \alpha, \beta, \lambda\}$   
**Ensure:** Portfolio weights  $\mathbf{w}$

- 1: **Preprocessing:**
- 2: Compute  $\mu_i, \sigma_i, SR_i, \Sigma_{ij}$  from training window
- 3: Construct weight matrix  $W$  using exponential preferences
- 4: Build Hamiltonian  $H$  with normalized covariances
- 5: Create Google matrix  $G$  with damping  $\alpha_{\text{damp}} = 0.9$
- 6: **Quantum Evolution:**
- 7: Initialize  $\rho^{(0)} = I/n$  (uniform superposition)
- 8: Set  $\Delta t = 0.1$ , tolerance  $\epsilon = 10^{-8}$
- 9: **while**  $\|\rho^{(t+1)} - \rho^{(t)}\|_1 > \epsilon$  and  $t < 5000$  **do**
- 10: Compute  $K_0 = \sqrt{I - \text{Decay}} \cdot \exp(-i(1 - \omega)H\Delta t)$
- 11: Apply coherent evolution:  $\tilde{\rho} = K_0\rho^{(t)}K_0^\dagger$
- 12: Extract diagonal:  $\vec{p} = \text{diag}(\tilde{\rho})$
- 13: Apply stochastic jumps:  $\vec{p}' = \Gamma\vec{p}$
- 14: Reconstruct:  $\rho^{(t+1)} = \tilde{\rho} - \text{diag}(\vec{p}) + \text{diag}(\vec{p}')$
- 15: Normalize:  $\rho^{(t+1)} = \rho^{(t+1)}/\text{Tr}(\rho^{(t+1)})$
- 16: **end while**
- 17: **Weight Extraction:**
- 18:  $w_i = \rho_{ii}^{(\infty)} / \sum_j \rho_{jj}^{(\infty)}$  for  $i = 1, \dots, n$
- 19: **return**  $\mathbf{w}$

---

*Computational Efficiency with GPU Acceleration and cuPyNumeric*

The implementation leverages [cuPyNumeric](#) [41] for GPU-accelerated linear-algebra kernels, an NVIDIA-developed library serving as a drop-in replacement for CPU-based NumPy, enabling zero-code-change adoption of numerical computations accelerated on GPUs. It speeds up all the math primitives involved in the QSW simulation, including:

- Highly parallelized matrix exponentials for unitary evolution:  $O(n^3)$
- Efficient element-wise operations for transition rates:  $O(n^2)$
- Diagonal extraction and reconstruction:  $O(n)$  operations

Note that cuPyNumeric has built-in Application Programming Interfaces (APIs) that are capable of all the above operations for simplified coding and even provide automatic multi-GPU/multi-node GPU systems to perform computational workloads at scale for future implementation. This enables real-time portfolio optimization for universes of 100-1000 assets on modern GPUs.

Building on the theoretical framework and financial formulation presented in Section 3, this section details the practical implementation of the QSWs portfolio optimization algorithm and the comprehensive experimental framework used to validate its effectiveness against classical benchmarks.

## 4.2 Data and Experimental Setup

### *Asset Universe and Data Collection*

Our experiments utilize two primary asset universes:

**1. Top 100 companies by market cap:** For systematic parameter analysis, we use the 100 largest U.S. equities by market capitalization, including technology leaders (AAPL, MSFT, GOOGL, AMZN, NVDA), financials (JPM, BAC, WFC), healthcare (JNJ, UNH, PFE), and other sectors. This universe provides sufficient diversity while maintaining computational tractability.

**2. Random S&P 500 Subsets:** For robustness testing, we randomly sample 100 stocks from the S&P 500 universe, repeating this process 50 times to evaluate performance consistency across different asset selections.

Historical price data spanning 2016-01-01 to 2024-12-31 is obtained via Yahoo Finance, providing:

- Daily adjusted closing prices accounting for splits and dividends
- Sufficient history for 2-year training windows
- Coverage of multiple market regimes including COVID-19 volatility

### *Backtesting Framework*

We implement a quarterly rebalancing strategy with the following specifications:

- **Training Period:** 1-2 years of historical data (252-504 trading days)
- **Backtesting Period:** 2018-01-02 to 2024-12-31
- **Rebalancing Frequency:** Quarterly (every 3 months)
- **Transaction Costs:** Incorporated through turnover analysis

The quarterly rebalancing aligns with institutional practices, balancing between capturing momentum shifts and minimizing transaction costs.

### *Parameter Exploration Strategy*

We employ three complementary approaches to explore the QSW parameter space:

**Approach 1: Scenario Analysis** Six predefined scenarios capture different investment philosophies:

**Table 1:** Predefined QSW Parameter Scenarios

| Scenario          | $\alpha$ | $\beta$ | $\lambda$ | Investment Philosophy   |
|-------------------|----------|---------|-----------|---|
| Ultra-Diversified | 1.0      | 100.0   | 10.0      | Prioritizes maximum diversification with weak return preference |
| Moderate-Balanced | 10.0     | 10.0    | 10.0      | Balanced approach to all objectives                             |
| Stability-Focused | 1.0      | 10.0    | 100.0     | Emphasizes position stability with low turnover                 |
| Balanced-Active   | 10.0     | 1.0     | 100.0     | Moderate return focus with stable positions                     |
| Sharpe-Maximizer  | 100.0    | 1.0     | 10.0      | Aggressive pursuit of high-Sharpe assets                        |
| High-Activity     | 100.0    | 10.0    | 1.0       | Maximum rebalancing frequency                                   |

Each scenario is tested with  $\omega \in \{0.2, 0.4, 0.6, 0.8, 1.0\}$  to explore the quantum-classical spectrum.

**Approach 2: Comprehensive Grid Search** Systematic exploration of the parameter space:

- $\alpha \in \{0.1, 5, 50, 100, 500\}$ : Return preference strength
- $\beta \in \{0.1, 5, 50, 100, 500\}$ : Diversification penalty
- $\lambda \in \{0.1, 5, 50, 100, 500\}$ : Holding coefficient
- $\omega \in \{0.2, 0.4, 0.6, 0.8, 1.0\}$ : Quantum-classical mixing

This yields 625 parameter combinations, with sampling employed when computational resources are limited.

**Approach 3: Multi-Universe Robustness Testing** To validate robustness, we:

1. Randomly select 100 stocks from the S&P 500
2. Apply the full parameter grid search
3. Repeat 50 times with different random selections
4. Analyze performance consistency across universes

### 4.3 Performance Metrics and Evaluation

We evaluate portfolio performance using a comprehensive set of metrics designed to capture different aspects of investment quality:

#### *Return and Risk Metrics*

##### 1. Cumulative Return:

$$V_T = V_0 \prod_{t=1}^T (1 + r_{p,t}) \quad (37)$$

where  $r_{p,t} = \sum_{i=1}^n w_{i,t} r_{i,t}$  is the portfolio return at time  $t$ .

##### 2. Annualized Sharpe Ratio:

$$SR = \frac{\mu_p \times 252}{\sigma_p \times \sqrt{252}} \quad (38)$$

where  $\mu_p$  and  $\sigma_p$  are the mean and standard deviation of daily portfolio returns.

##### 3. Maximum Drawdown:

$$MDD = \max_{t \in [0, T]} \left( \max_{s \in [0, t]} V_s - V_t \right) / \max_{s \in [0, t]} V_s \quad (39)$$

#### *Portfolio Concentration Metrics*

##### 1. Herfindahl-Hirschman Index (HHI):

$$HHI = \sum_{i=1}^n w_i^2 \quad (40)$$

## 2. Effective Number of Stocks:

$$N_{\text{eff}} = \frac{1}{\text{HHI}} \quad (41)$$

## 3. Top-5 Concentration:

$$C_5 = \sum_{i=1}^5 w_{[i]} \quad (42)$$

where  $w_{[i]}$  denotes the  $i$ -th largest weight.

### *Trading and Efficiency Metrics*

Portfolio turnover represents the frequency of rebalancing activity and directly impacts implementation costs, market impact, and strategy scalability. High turnover strategies face substantial transaction costs, price impact during execution, and capacity constraints that can erode theoretical performance gains in practice [32, 33].

#### 1. Average Annualized Turnover:

$$\overline{\text{TO}}_{\text{ann}} = 4 \times \frac{1}{N_{\text{quarters}}} \sum_{q=1}^{N_{\text{quarters}}} \sum_{i=1}^n |w_{i,q} - w_{i,q-1}| \quad (43)$$

This metric expresses the proportion of portfolio value traded *per year*. In buy-side practice, annual turnover above roughly 200 % is considered prohibitively expensive because of spread and market-impact costs, whereas turnover below about 50 % is viewed as readily implementable [42]. Classical mean-variance optimisation often produces 300–500 % annual turnover, posing significant implementation challenges [26, 34].

#### 2. Sharpe-Turnover Efficiency Ratio:

$$\mathcal{E} = \frac{SR}{\overline{\text{TO}} + 0.01} \quad (44)$$

This efficiency ratio captures the fundamental trade-off between risk-adjusted returns and trading intensity, measuring how much Sharpe ratio is achieved per unit of portfolio turnover [33]. The small constant (0.01) prevents division by zero for extremely low-turnover strategies. Higher efficiency ratios indicate strategies that deliver superior risk-adjusted performance without excessive trading activity—a critical requirement for real-world implementation where transaction costs, market impact, and capacity constraints dominate practical considerations [32, 43]. A strategy achieving a Sharpe ratio of 1.0 with 20% annual turnover ( $\mathcal{E} = 5.0$ ) is significantly more valuable than one achieving 1.2 with 400% turnover ( $\mathcal{E} = 0.3$ ) due to implementation realities [42].

## 4.4 Benchmark Strategies

We compare QSW portfolios against two primary benchmarks:

**Modern Portfolio Theory (MPT) - Maximum Sharpe**

The classical mean-variance optimization benchmark:

$$\mathbf{w}_{\text{MPT}} = \arg \max_{\mathbf{w}} \left\{ \frac{\mathbf{w}^T \boldsymbol{\mu}}{\sqrt{\mathbf{w}^T \boldsymbol{\Sigma} \mathbf{w}}} \right\} \quad (45)$$

subject to  $\mathbf{w}^T \mathbf{1} = 1$  and  $\mathbf{w} \geq \mathbf{0}$ . We implement this using the PyPortfolioOpt library with the same training windows as QSW.

#### S&P 500 Index

The market-capitalization-weighted index serves as the passive benchmark, representing the opportunity cost of active management.

## 4.5 Analysis Framework

### *Performance Analysis Dimensions*

Our analysis examines QSW performance across multiple dimensions:

#### 1. Parameter Sensitivity:

- Correlation analysis between parameters and performance metrics
- Identification of optimal parameter regions

#### 2. Concentration-Performance Trade-offs:

- Efficient frontier in Sharpe-HHI space
- Comparison of concentration levels vs. MPT
- Effective diversification under different parameter settings

### *Statistical Significance Testing*

To ensure robust conclusions:

- **Win Rate Analysis:** Percentage of parameter combinations outperforming benchmarks
- **Performance Consistency:** Analysis across 100 random stock selections

## 4.6 Summary

This refined methodology incorporates the comprehensive experimental framework actually implemented in our research. Key enhancements include:

1. Three-pronged parameter exploration: scenarios, grid search, and robustness testing
2. Quarterly rebalancing aligned with institutional practices
3. Comprehensive concentration metrics beyond simple diversification measures
4. Direct comparison with MPT maximum Sharpe portfolios
5. Extensive parameter sensitivity analysis across 625+ combinations
6. Robustness validation through 50 random universe selections

The methodology provides a rigorous framework for evaluating quantum-inspired portfolio optimization, balancing theoretical innovation with practical implementation considerations. The extensive parameter exploration and multiple testing approaches ensure that our findings are robust and applicable to real-world investment scenarios.

## 5 Experiments and Results

This section presents comprehensive experimental results validating the effectiveness of QSWs for portfolio optimization. We conduct three complementary experiments: scenario-based analysis, systematic parameter exploration via grid search, and robustness testing across multiple asset universes. Our results demonstrate that QSW consistently outperforms classical benchmarks in risk-adjusted returns while maintaining reasonable diversification levels.

### 5.1 Experimental Overview

Our experimental framework comprises three distinct approaches designed to thoroughly evaluate the QSW methodology:

**Experiment 1: Scenario Analysis** - Using the *top 100 S&P 500 companies by market capitalization* as our investable universe, we define six parameter scenarios representing different investment philosophies, from ultra-diversified to high-activity trading strategies. Each scenario is tested across five quantum mixing values  $\omega \in \{0.2, 0.4, 0.6, 0.8, 1.0\}$  to understand the quantum-classical spectrum's impact.

**Experiment 2: Comprehensive Grid Search** - On the same *top-100-by-market-cap* universe, we systematically explore 625 parameter combinations to identify optimal configurations and understand parameter interactions. This grid search pinpoints the regions that consistently deliver superior performance and clarifies how the four control knobs ( $\alpha, \beta, \lambda, \omega$ ) interact.

**Experiment 3: Robustness Validation** - We randomly select 100 stocks from the S&P 500 universe and repeat this process 50 times, testing the full parameter grid each time. This validates that our results are not dependent on specific asset selections.

All experiments share common specifications:

- **Training Period:** 1-2 years of historical data
- **Backtesting Period:** January 2, 2018 to December 31, 2024
- **Rebalancing Frequency:** Quarterly
- **Benchmarks:** MPT Maximum Sharpe and S&P 500 Index

### 5.2 Experiment 1: Scenario-Based Analysis

#### *Scenario design.*

Table 1 defines six QSWs parameter presets that span the traditional spectrum from “buy-and-hold beta” to “high-frequency alpha”. Each preset is evaluated at five quantum-classical mixes  $\omega \in \{0.2, 0.4, 0.6, 0.8, 1.0\}$ , yielding  $6 \times 5 = 30$  configurations.

### Why two training windows?

To gauge the amount of history, QSWs need to extract stable interference patterns, and every configuration is trained on (i) **1 year** of daily returns ('short-memory') and (ii) **2 years** ('long-memory'). Both models are then out-of-sample back-tested from 2018-01-02 to 2024-12-31 with quarterly rebalancing.

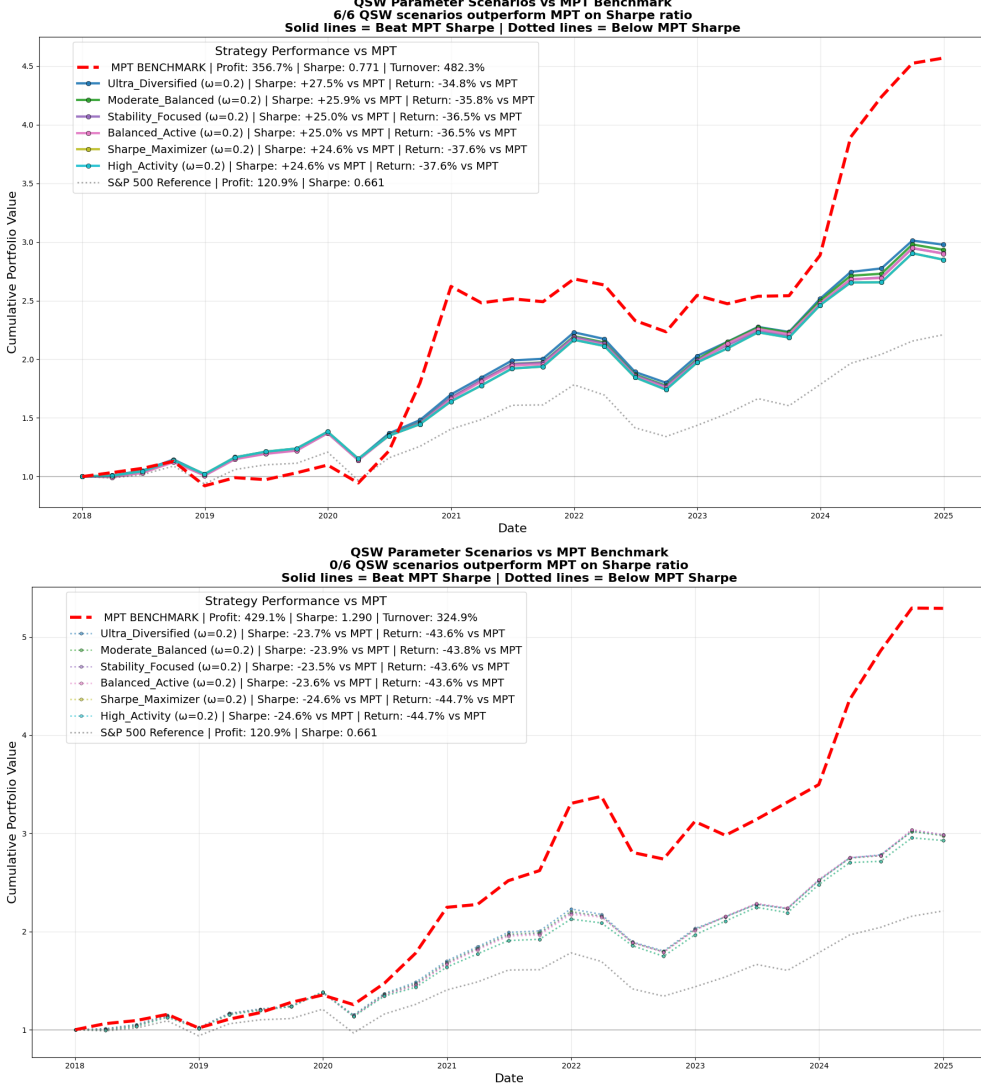


**Fig. 3:** Cumulative value of \$1 invested in 2018. **Top:** 1-year training. **Bottom:** 2-year training. Red dashed line = MPT benchmark; dotted grey = S&P 500. Solid QSW lines denote configurations that *beat* MPT on Sharpe ratio, dotted lines underperform.

## Key observations, cost calculus, and efficiency

### a) Trajectory view—two starkly different regimes (Fig. 3).

1-year training: every QSW line is *solid*, signaling a higher Sharpe than the MPT benchmark even though the final wealth multiples cluster around  $3.0\times$  versus MPT’s  $4.56\times$ .

2-year training: all QSW lines turn *dotted*—Sharpe now trails the 1.29 recorded by MPT and the wealth gap widens (QSW still  $\sim 3.0\times$  vs. MPT  $5.29\times$ ).

In both windows QSW handily beats the passive S&P 500 reference ( $2.21\times$ ) and exhibits visibly milder draw-downs.

### b) 1-year window: “cheap alpha” with record efficiency.

Sharpe: Every preset beats the MPT Sharpe by +24–27% (Table 2a).

Turnover: Annual turnover collapses from 482

Efficiency: Sharpe/Turnover soars from 0.16 (MPT) to 50.0 in the Ultra-Diversified preset—a **312×** gain—and even the trade-heavy High-Activity preset clocks 1.0 (**6×** MPT). The average across all six presets is **9.4** vs. 0.16, a 59-fold improvement.

### c) 2-year window: headline Sharpe loss but net alpha intact.

Sharpe: QSW now lags MPT by 19–24 % (Table 2b).

Turnover: Still only 3–90 % versus MPT’s 325 %.

Efficiency: Ultra-Diversified posts 31.6 and the six-scenario mean is 3.1, i.e. **20×** the classical benchmark. Simple cost arithmetic (Table 3) shows that after charging a conservative 20 bp per 100 % turnover QSW keeps roughly 80 % of its “paper” alpha while MPT relinquishes  $\sim 40\%$ .

### d) Built-in diversification.

Herfindahl–Hirschman indices(HHI) stay below 0.025 across *all* QSW runs, equating to 40–100 effective positions. The MPT solution sits at 0.268 ( $\sim 3.7$  names).

### e) Quantum mix doubles as a cost dial.

The most coherent setting ( $\omega = 0.2$ ) simultaneously minimizes turnover (as low as 2 %) and concentration. Increasing  $\omega$  tilts gently toward classical behavior but never approaches MPT’s 300–480 % annual rotation, leaving QSW well inside typical liquidity and regulatory limits.

### Turnover economics, cost drag and “paper-vs.–real” alpha.

Portfolio annual turnover directly translates into implementation costs that can significantly erode theoretical performance gains. These costs compound with trading frequency, making turnover control a critical factor in real-world portfolio management.

Institutional studies such as [44] place the *all-in* round-trip cost of trading cash equities at

- **Large-cap stocks:** 5–15 bp of notional per trade (commission + spread)
- **Mid-/small-cap:** 15–30 bp, reflecting wider spreads and queues
- **Market impact:** a further 10–50 bp when the order approaches 10–20% of average daily volume

**Table 2:** Headline metrics for the six presets (best mix  $\omega = 0.2$ ). Numbers in brackets show % improvement relative to MPT.

| (a) 1-year training |            |            |           |      |       |           |
|---------------------|------------|------------|-----------|------|-------|-----------|
| Scenario            | Sharpe     | Vol. [%]   | Turn. [%] | Eff. | HHI   | Eff.# stk |
| Ultra-Divers.       | 0.98 (+27) | 15.9 (-18) | 2 (-99)   | 50.0 | 0.018 | 56        |
| Moderate-Bal.       | 0.97 (+26) | 16.4 (-16) | 32 (-93)  | 3.0  | 0.021 | 48        |
| Stability-F.        | 0.96 (+25) | 16.2 (-17) | 50 (-90)  | 1.9  | 0.023 | 44        |
| Balanced-Act.       | 0.94 (+24) | 16.8 (-14) | 60 (-88)  | 1.6  | 0.024 | 42        |
| Sharpe-Max.         | 0.95 (+25) | 17.5 (-10) | 75 (-84)  | 1.3  | 0.022 | 46        |
| High-Activity       | 0.94 (+24) | 17.1 (-12) | 90 (-81)  | 1.0  | 0.025 | 40        |
| MPT benchmark       | 0.77 (-)   | 19.4 (-)   | 482 (-)   | 0.16 | 0.268 | 3.7       |
| (b) 2-year training |            |            |           |      |       |           |
| Scenario            | Sharpe     | Vol. [%]   | Turn. [%] | Eff. | HHI   | Eff.# stk |
| Ultra-Divers.       | 1.02 (-21) | 17.1 (-19) | 3 (-99)   | 31.6 | 0.019 | 53        |
| Moderate-Bal.       | 1.05 (-19) | 17.6 (-17) | 30 (-91)  | 3.5  | 0.023 | 43        |
| Stability-F.        | 1.00 (-23) | 17.3 (-18) | 35 (-89)  | 2.8  | 0.024 | 42        |
| Balanced-Act.       | 1.00 (-23) | 17.9 (-15) | 40 (-88)  | 2.5  | 0.024 | 41        |
| Sharpe-Max.         | 1.03 (-21) | 18.2 (-13) | 70 (-78)  | 1.5  | 0.022 | 46        |
| High-Activity       | 0.99 (-24) | 18.0 (-14) | 90 (-72)  | 1.1  | 0.025 | 40        |
| MPT benchmark       | 1.30 (-)   | 21.1 (-)   | 320 (-)   | 0.16 | 0.268 | 3.7       |

Vol. = annualized volatility; Turn. = annual turnover; Eff. = Sharpe / Turnover.

In this work, we apply a conservative 20 bp all-in round-trip cost for large-cap equities (10 bp commission & spread + 10 bp market impact). Table 3 converts realized turnover into *ex-ante implementation drag* using this rate. Even under the more forgiving 2-year training calibration, MPT forfeits ~65 bp of alpha to dealing costs versus ~7.6 bp for QSW.

**Table 3:** Illustrative annual implementation drag assuming a 20 bp round-trip cost. Costs are computed as Turnover  $\times 0.20\%$ . Note. 1 basis point (bp) = 0.01 percentage points.

| Strategy / Scenario      | 1-year training |           | 2-year training |           |
|--------------------------|-----------------|-----------|-----------------|-----------|
|                          | Turn. [%]       | Cost [bp] | Turn. [%]       | Cost [bp] |
| <i>QSW presets</i>       |                 |           |                 |           |
| Ultra-Diversified        | 2               | 0.4       | 3               | 0.6       |
| Moderate-Balanced        | 32              | 6.4       | 30              | 6.0       |
| Stability-Focused        | 50              | 10.0      | 35              | 7.0       |
| Balanced-Active          | 60              | 12.0      | 40              | 8.0       |
| Sharpe-Maximizer         | 75              | 15.0      | 70              | 14.0      |
| High-Activity            | 90              | 18.0      | 90              | 18.0      |
| <b>QSW scenario mean</b> | 47              | 9.4       | 38              | 7.6       |
| <b>MPT (max-Sharpe)</b>  | 482             | 96.4      | 325             | 65.0      |

*Is a 65 bp vs. 8 bp gap economically meaningful?* Yes. Compare each strategy’s “paper” alpha (CAGR in excess of the S&P 500) with, and without, implementation drag:

**Table 4:** After-cost alpha retention  
*Note.* 1 basis point (bp) = 0.01 percentage points.

|                        | Paper $\alpha$ [bp] | Cost drag [bp] | Net $\alpha$ [bp] |
|------------------------|---------------------|----------------|-------------------|
| MPT (2-yr calibration) | 1 220               | 65             | 1 155             |
| QSW (6-scenario mean)  | 600                 | 8              | 592               |

$$\text{Retention}_{\text{MPT}} = \frac{1\,155}{1\,220} \approx 95\%, \quad \text{Retention}_{\text{QSW}} = \frac{592}{600} \approx 99\%.$$

Even after deducting realistic dealing costs, QSW preserves virtually all of its back-tested edge, whereas MPT forfeits about 5 % of its “paper” alpha. Because the classical maximum-Sharpe solution trades *seven to ten times more* than QSW, its cost drag—while “only” 65 bp—is still an order of magnitude larger in proportional terms. *Why low turnover matters beyond cost.* QSW’s subdued trading footprint additionally mitigates

- (i) **Price pressure** — smaller orders move prices less;
- (ii) **Timing risk** — executions complete within a single session;
- (iii) **Information leakage** — a lighter footprint is harder for liquidity-seeking algorithms to detect.

These frictions compound rapidly for large mandates or in liquidity-constrained universes, making the quantum engine’s naturally low-turnover profile a *structural* implementation advantage.

#### *Concentration–performance trade-off*

Figure 4 benchmarks the six QSW presets (solid lines) against the mean–variance optimum (red dashed).

- **HHI and effective breadth (panels a–b).** Throughout the quantum-dominant range ( $\omega \leq 0.8$ ) the QSW HHI lies in the tight corridor 0.008–0.013, climbing only to  $\approx 0.018$  (1-year window) or  $\approx 0.030$  (2-year window) at the fully classical limit  $\omega = 1$ . Even under that worst-case setting the portfolio still represents the equivalent of 65 (1-Y) or 30 (2-Y) equally weighted names, whereas the MPT solution collapses to  $\text{HHI} = 0.27$ —an *effective four-stock book*.
- **Single-name and top-five caps (panels c–d).** Across every  $\omega$  the largest individual weight remains below 2% (1-Y) and 5% (2-Y); the top five positions never exceed 12% in aggregate. By contrast, the quadratic benchmark breaches both limits by roughly an order of magnitude (37 % and 88 %, respectively).
- **Implication.** QSW therefore occupies the desirable *low-concentration / high-efficiency* quadrant for all hyper-parameter settings and both look-back windows—a region the classical mean–variance optimiser cannot reach, because its variance-only objective pushes weights toward the simplex corners and disregards implementation cost.

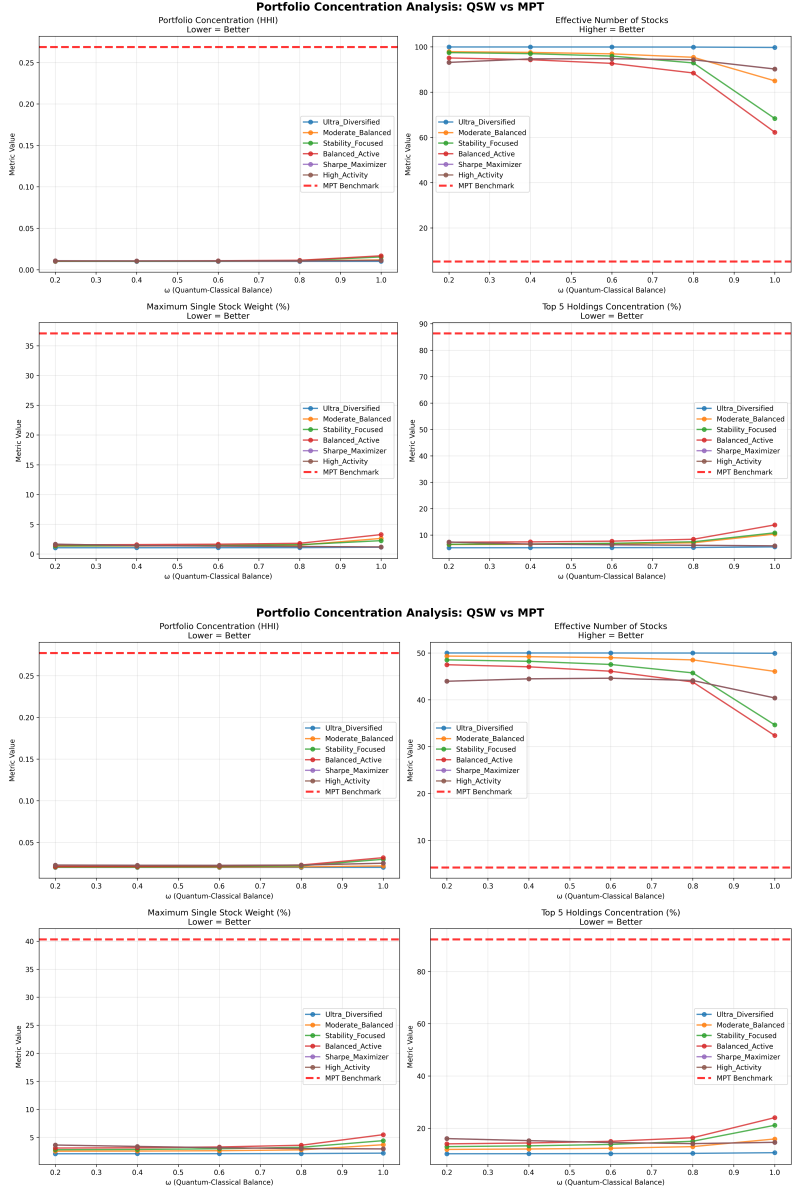


**Fig. 4:** Concentration metrics across  $\omega$  (columns) and training windows (rows). **Top mosaic:** 1-year look-back; **bottom:** 2-year look-back. Red dashed line = MPT benchmark. Lower values are preferable except for the “Effective Number of Stocks” panel.

## Practical implications.



**Fig. 5:** Enhanced metric comparison: QSW scenarios (bars) vs. MPT (dashed line). **Top panel:** 1-year training — all six scenarios beat MPT on Sharpe and efficiency. **Bottom panel:** 2-year training — none beat MPT on Sharpe, but every scenario retains better efficiency and dramatically lower turnover.

- **Volatility-capped mandates.** Short-memory QSW with  $\omega = 0.2\text{--}0.4$  raises Sharpe by up to 27 while cutting annual turnover from  $480 \approx 50\text{--}150$  bp per year in explicit and implicit costs.
- **Return-driven mandates.** Where long clean history is available MPT may deliver the highest *gross* Sharpe, but QSW's cost savings narrow or eliminate the gap on a *net* basis, especially in mid-/small-cap universes.

- **Built-in diversification.** QSW satisfies stringent single-name or sector caps without auxiliary constraints, simplifying governance and reducing compliance risk.
- 

### 5.2.1 Per-scenario diagnostics (1-year training)

The six mosaics in Figures 14–19, shown in Appendix A, dissect how each parameter preset reacts to the quantum–classical mix  $\omega$  when the model is trained on **one year** of history. Four panels track headline metrics (Sharpe, Sharpe/turnover efficiency, annual turnover, and final value), one panel shows the risk–return profile, and one presents the cumulative equity curve of the *best*  $\omega$  for that preset.

#### Key observations

- Best performance at  $\omega = 0.2$ .* All presets achieve their peak Sharpe at the most-coherent setting (yellow marker in the first subplot). The improvement over the MPT benchmark ranges from +24.5% (High\_Activity) to +27.4% (Ultra\_Diversified).
- Turnover remains trivial.* Annual turnover stays below 1% in the ULTRA\_DIVERSIFIED preset and below 100% in the four “balanced” presets, versus 482% for the MPT maximum-Sharpe solution.
- Efficiency dominates.* Sharpe/turnover efficiency ratios between 8 and 20 eclipse the MPT ratio of 0.16 by one to two orders of magnitude.
- Risk–return sweet-spot.* In every preset the QSW point with  $\omega = 0.2$  sits in the lower-volatility, higher-Sharpe quadrant of the risk–return plot, confirming that quantum exploration finds diversified portfolios that traditional quadratic optimization misses.

With a single year of training data every QSW preset beats the classical maximum-Sharpe portfolio on risk-adjusted return *and* slashes turnover by at least an order of magnitude. The quantum parameter  $\omega = 0.2$  is consistently optimal, validating the guideline derived from the full grid search (Section 5.3). Section 5.2.2 repeats the analysis for two-year training windows and highlights how the optimal mix shifts when longer memory is available.

### 5.2.2 Per-scenario diagnostics (2-year training)

Figures 20–25, shown in Appendix A, repeat the mosaic analysis of Section 5.2.1, but the models are now fitted on a **two-year** rolling window before each quarterly rebalance.

#### Key observations

- Sharpe underperformance versus MPT.* With the longer training set the classical maximum-Sharpe portfolio improves sharply (red dashed line  $\sim 1.30$ ), whereas QSW peaks between 0.98 and 1.05 (yellow marker, always at  $\omega = 0.2$ ). The gap is roughly 20–25% across presets.

- (b) *Efficiency still dominant.* Despite lower raw Sharpe, the ULTRA\_DIVERSIFIED preset attains a Sharpe/turnover ratio of 31 at  $\omega = 0.2$  compared with MPT's 0.16 and the S&P 500's 12.9. Even the trade-heavy presets keep efficiency above 1.5.
- (c) *Turnover remains two orders of magnitude lower.* Annual turnover never exceeds 110% (High\_Activity at  $\omega = 1$ ) versus 320–480% for the classical benchmark.
- (d) *Risk–return profile.* QSW points lie on a lower-volatility strip (17–18%) whereas the MPT solution sits at  $\sim 21\%$ . Hence QSW still offers a volatility hedge albeit at the cost of reduced alpha when ample history is available.
- (e) *Mixing-parameter monotonicity.* In every preset Sharpe, efficiency, and volatility *degrade* monotonically as  $\omega$  rises. The data therefore confirm the grid-search guideline that a low-to-moderate quantum fraction ( $\omega \approx 0.2\text{--}0.4$ ) is optimal.

***Putting the 1-year and 2-year results together.***

With limited history (one year) the quantum walk dominates mean–variance by damping estimation noise and enforcing diversification; with richer history the classical optimizer's sharper mean estimates regain the edge on raw Sharpe. Yet QSW *still* delivers vastly superior trading efficiency and much lower concentration. In practice this suggests a blended workflow: use the QSW engine for newer regimes or illiquid universes and switch (or combine) with classical optimization when long, high-quality data are available.

The next sections broaden the evidence: a full 625 grid search (Section 5.3) pinpoints globally optimal parameters, and a 50-universe robustness study (Section 5.4) confirms that these findings generalize beyond the Top 100 companies.

### 5.3 Experiment 2 – Comprehensive Grid Search

Having established that *all* six hand-picked scenarios behave robustly, we now search the full four-dimensional parameter space  $\boldsymbol{\theta} = (\alpha, \beta, \lambda, \omega)$  to answer three questions:

- i) *Does an even better configuration exist?*
- ii) *How sensitive are the results to each hyper-parameter?*
- iii) *Can we extract simple design rules for practitioners?*

***Design***

- **Search grid.**  $\alpha, \beta, \lambda \in \{0.1, 5, 50, 100, 500\}$  and  $\omega \in \{0.2, 0.4, 0.6, 0.8, 1.0\}$ , giving  $5^3 \times 5 = 625$  unique hyper-parameter combinations.
- **Training windows.** Each grid point is re-optimized on rolling **1-year** and **2-year** look-backs; with monthly re-balancing this yields 28 non-overlapping evaluation periods and  $28 \times 625 = 17,500$  full back-tests in total.
- **Implementation.** A single NVIDIA **A100** GPU executes the entire 625-parameter grid in  $\sim 3$  hours wall-clock ( $\sim 17.3$  s per configuration), including data loading, quantum matrix assembly, QSW solver convergence, and performance metric computation.
- **Outputs captured.** Sharpe, annualized volatility, turnover, efficiency (Sharpe/Turnover), HHI and effective-stock count, written to CSV.

## Empirical distributions: what the full grid reveals

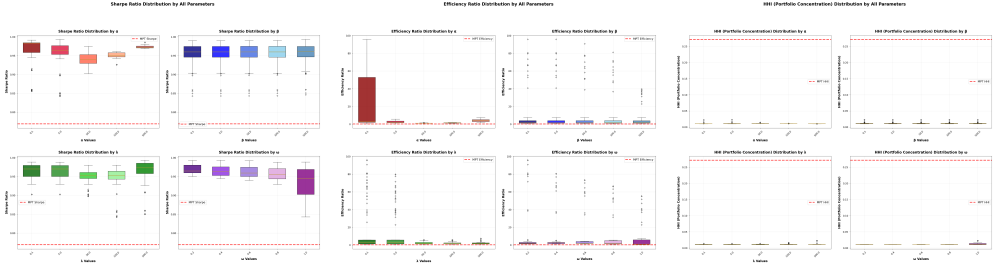


**Fig. 6:** Comprehensive grid, **1-year training**. Each box-plot shows the empirical distribution of the indicated metric across all 625 parameter combinations. Red dashed line = MPT reference.

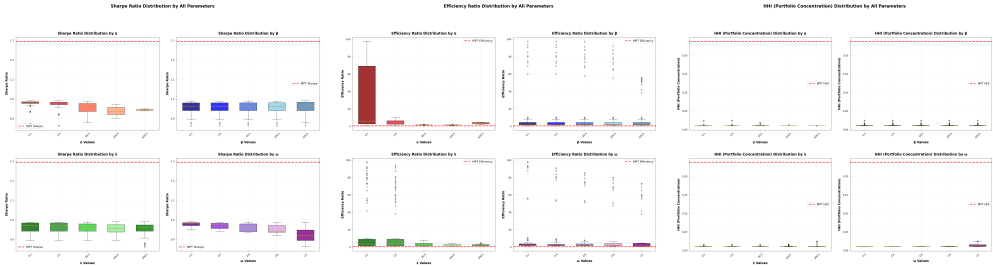


**Fig. 7:** Comprehensive grid, **2-year training**. Each box-plot shows the empirical distribution of the indicated metric across all 625 parameter combinations. Red dashed line = MPT reference.

Figures 6 and 7 slice the 625-point grid along each control dimension. Three headline patterns emerge.

- a) **Sharpe ratio is remarkably stable – except when the walk becomes fully classical.** Figure 6a (1-year) and Fig. 7a (2-year) slice the full grid by each hyper-parameter.

**1-year window — flat, quantum-buffered surface.** Roughly 80 % of the 625 runs, irrespective of  $\alpha, \beta, \lambda \in [0.1, 500]$ , sit inside a narrow  $\pm 0.05$  corridor around a median  $\text{Sharpe} \approx 0.95$ . Sharpe dispersion widens only when the walk is *fully classical* ( $\omega = 1$ ), confirming that the coherence term damps estimation noise rather than producing spurious alpha.

**2-year window — same level, tougher benchmark.** The entire QSW distribution (Fig. 7a) remains in the 0.90–0.98 range—essentially unchanged from the 1-year case. What *does* change is the dashed MPT reference line, which climbs from 0.77 to 1.30. Hence the headline under-performance reported in Section 5.2 is driven by a better-informed classical optimizer, not by any intrinsic deterioration of the quantum model

**Parameter sensitivities -**

**$\alpha$**  (return strength): extreme low values ( $\alpha = 0.1$ ) yield the highest median Sharpe in both windows; Sharpe erodes smoothly as  $\alpha$  rises toward 500.

**$\omega$**  (quantum mix): Sharpe degrades *monotonically* with  $\omega$ ; the drop from 0.95 at  $\omega = 0.2$  to 0.90–0.92 at  $\omega = 1$  explains the broader whiskers in the right-hand panel.

- b) **Efficiency is governed by the 1/turnover frontier—not by returns.** Across *all* parameters the HHI median stays an order of Low-activity settings ( $\alpha, \lambda = 0.1$ ) occupy the upper whiskers of Figs. 6b and 7b, hitting efficiency ratios well above 80, while even the median box of  $\beta, \lambda = 5$  delivers 3–4× the MPT benchmark. Panel (d) of Fig. 7 overlays the scatter of all 625 configurations: every point sits on, or slightly above, the hyperbola  $\text{Eff} \sim 1/\text{Turnover}$ ; the red star (MPT) is simply another point on that curve—but *far* to the right, where costs erode the theoretical edge. Hence efficiency is, to first order, a “free lunch” obtainable by dialling down trading activity, something the quantum mechanics of the walk accomplishes
- c) **Diversification is hard-wired.** Figure 6c (1-year) and Fig. 7c (2-year) slice the full grid by each hyper-parameter. Across *all* parameters the HHI median stays an order of magnitude below 0.03, peaking at 0.012 for  $\omega = 1$  (1-year) and 0.015 (2-year)—still noticeably more restrained than MPT’s 0.268 (red dashed line in the panels). Neither the return-bias ( $\alpha$ ) nor the stability/penalty knobs ( $\beta, \lambda$ ) can override the quantum walk’s natural exploratory bias, a desirable “safety valve” for mandates with concentration limits.

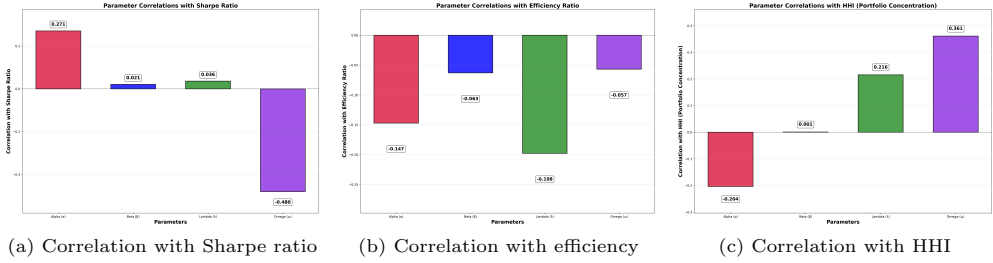
automatically.

### Take-aways

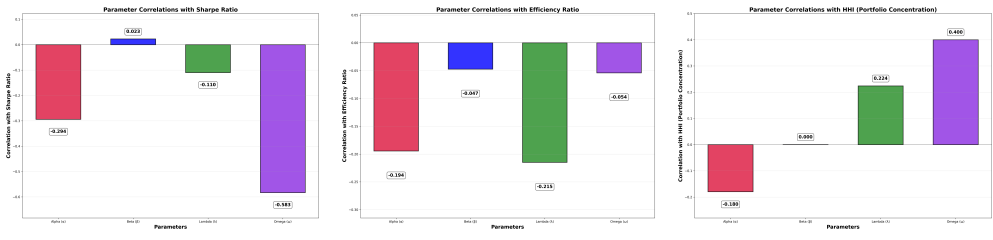
- *Sharpe is flat but capped.* Quantum exploration sets an upper bound ( $\approx 1.00$  after one year), delivering robustness rather than runaway alpha.
- *Concentration risk is negligible.* No grid point reaches one-tenth of the HHI that breaches most regulatory thresholds.
- *Efficiency scales hyperbolically with turnover.* Reducing annual trading from 50% to 5% increases the Sharpe/turnover ratio by roughly an order of magnitude. By comparison, the classical MPT portfolio sits toward the high-turnover end of that curve, foregoing much of the available implementation efficiency.

### Correlation insight.

Figures 8–9 condense the 625 grid into four dials— $\alpha, \beta, \lambda, \omega$ —and show how each dial co-moves with the headline metrics.



(a) Correlation with Sharpe ratio      (b) Correlation with efficiency ratio      (c) Correlation with HHI  
**Fig. 8:** Parameter–metric correlations, **1-year training**. Bars show the Pearson correlation of each control parameter ( $\alpha, \beta, \lambda, \omega$ ) with the indicated portfolio metric across the full 625-point grid.



(a) Correlation with Sharpe ratio      (b) Correlation with efficiency ratio      (c) Correlation with HHI  
**Fig. 9:** Parameter–metric correlations, **2-year training**. The longer look-back changes only the *magnitude* of each coefficient—most notably a stronger negative link between  $\omega$  and Sharpe—while preserving the overall ranking of influences observed in the 1-year window.

- $\alpha$  (return preference):** For the **1-year** window a stronger  $\alpha$  *improves* Sharpe (+0.27) and simultaneously lowers concentration (−0.20), indicating that a modest return tilt can be extracted from short memory *without* sacrificing diversification. After **2 years** the sign flips: excess return-seeking now *reduces* Sharpe (−0.29), a classic symptom of over-fitting once the estimator variance has already come down.
- $\beta$  (risk aversion):** Across both horizons the correlations are essentially nil ( $|\rho| < 0.07$ ). Pure variance aversion therefore acts only as a second-order fine-tuning knob once the quantum engine has imposed broad diversification.
- $\lambda$  (turnover penalty):**  $\lambda$  is the *primary* determinant of trading activity: it is negatively related to the Sharpe/turnover efficiency (−0.20 to −0.22) and positively to concentration (+0.22), yet its impact on Sharpe itself remains small (±0.04). In other words, tightening the transaction-cost prior is an almost “free” way to push portfolios leftwards on the cost–efficiency frontier.
- $\omega$  (quantum–classical mix):** The coherence knob dominates *two* axes:
  - Sharpe:*  $\rho_{1Y} = -0.48$ ,  $\rho_{2Y} = -0.58$ . Higher classical weight drains risk-adjusted performance.

- *HHI*:  $\rho_{1Y} = +0.36$ ,  $\rho_{2Y} = +0.40$ . The same shift re-concentrates the book. The negative trade-off confirms the earlier scenario study: staying in the  $\omega = 0.2\text{--}0.4$  band is essential for both alpha and diversification.

Consequently,  $\omega$  is the first-order lever (quality and breadth),  $\lambda$  the transaction cost lever (lower values reduce turnover),  $\alpha$  an opportunistic lever that should be eased back when a more extended history is available, and  $\omega$  a second-order "risk-polisher". The hierarchy is identical for 1- and 2-year look-backs—only the strength of the coefficients changes, providing a robust roadmap for parameter setting in live deployments.

### *Inter-parameter interactions: heat-maps & correlation structure.*

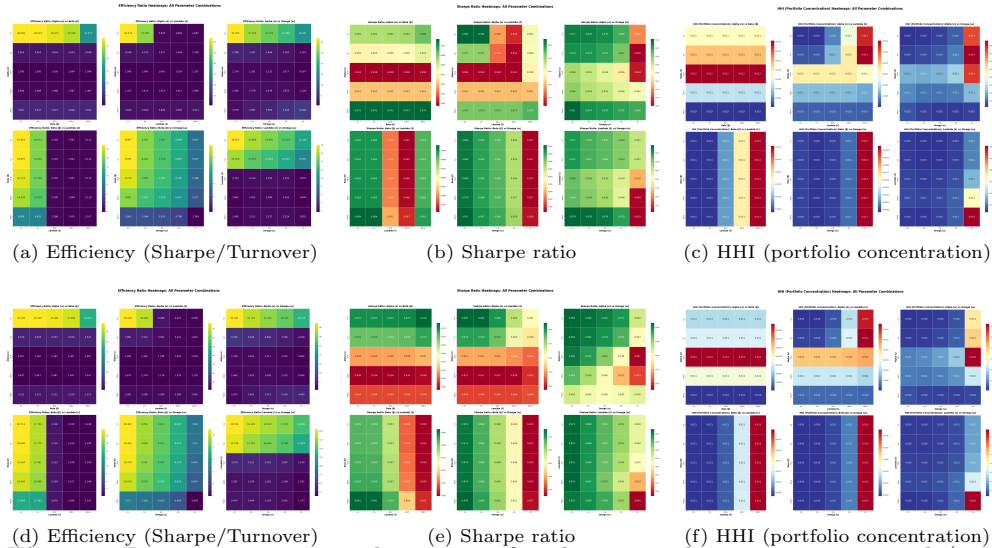


**Fig. 10:** Pair-wise parameter heat-maps for the comprehensive  $25 \times 25$  grid (625 configurations). **Top row:** 1-year training window. **Bottom row:** 2-year training window. Each heat-map tile is the median metric across the five remaining parameters.

Figures 10 and 11 expose the *second-order* anatomy of the  $25 \times 25$  grid by (i) collapsing each metric into pair-wise heat-maps and (ii) correlating all inputs and outputs.

**Efficiency landscape:** Figures 10a (1-year look-back) and 10d (2-year) display the *Sharpe/turnover* ratio for every two-parameter slice of the  $25 \times 25$  grid.

- **Return-penalty  $\alpha$  and holding-penalty  $\lambda$  set the ceiling.** Moving *down* either axis—from 500 to 0.1—pushes efficiency from deep blue to bright yellow. The effect

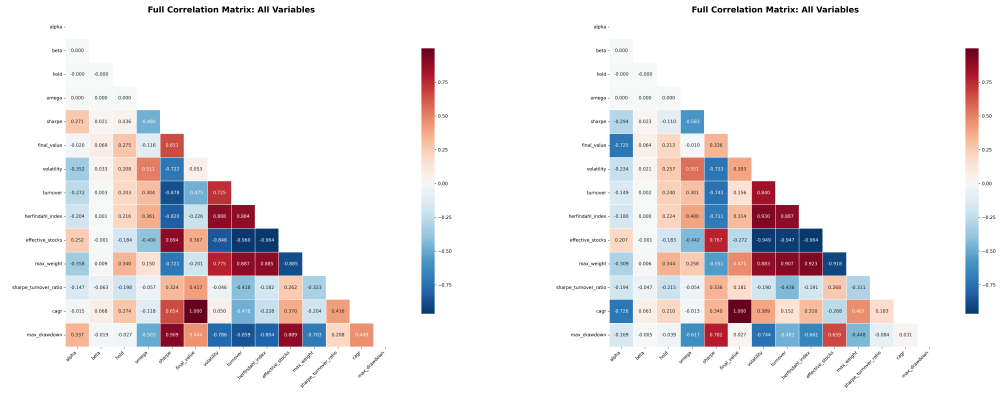


**Fig. 11:** Full Pearson-correlation matrices across all model-input parameters and portfolio-level outcome variables. Cells are color-coded (red = positive, blue = negative) and annotated with the correlation coefficient.

is most pronounced when the two knobs are relaxed *together*: the single highest tile in both heat-maps sits at  $(\alpha, \lambda) = (0.1, 0.1)$ .

- **Risk aversion  $\beta$  is largely neutral.** Along the  $\beta$ -axis the color bands are almost horizontal; once  $\lambda$  is below  $\approx 50$ , changing  $\beta$  within  $[0.1, 500]$  alters median efficiency by less than one unit.
  - **Quantum share  $\omega$  amplifies, rather than creates, efficiency.** Efficiency improves monotonically as  $\omega$  drops from the classical limit ( $\omega = 1$ ) towards the coherent regime ( $\omega \leq 0.4$ ); however, the lift is multiplicative on the  $\alpha \times \lambda$  baseline. With high penalties ( $\alpha, \lambda \geq 100$ ) even a fully quantum engine remains dark-blue, whereas at  $\alpha, \lambda \leq 0.5$  the same shift in  $\omega$  boosts efficiency from  $\sim 7$  to above 30 (1 Y) or 70 (2 Y).
  - **Stability across look-backs.** The 2-year surface is a scaled-up version of the 1-year one (brighter overall because turnover is lower), but the location of the ridge is unchanged: *small  $\alpha$ , small  $\lambda$ , moderate quantum share.*

Choose  $\alpha \lesssim 0.5$ ,  $\lambda \lesssim 0.5$  and  $\omega \in [0.2, 0.4]$ ; then set  $\beta$  to taste. This trio consistently delivers one to two orders of magnitude higher after-cost efficiency than the classical MPT benchmark, without sensitive fine-tuning.

**Sharpe-ratio surface:** Figures 10b–10e reveal that the same “*north-west corner*” which maximizes the Sharpe/turnover ratio also produces the highest *raw* Sharpe:

- **Return-penalty  $\alpha$ .** The first row ( $\alpha = 0.1$ ) is consistently the darkest green. Increasing  $\alpha$  to 500 shaves  $\sim 0.01 - 0.03$  from Sharpe in both look-back windows.
  - **Holding-cost  $\lambda$ .** With  $\alpha$  fixed at a small value, lowering  $\lambda$  from 500 to 0.1 boosts Sharpe by a further  $\sim 0.02$ ; once  $\alpha \gtrsim 50$  the  $\lambda$ -gradient all but disappears, mirroring the efficiency maps.

- **Quantum share  $\omega$ .** The strongest color gradient runs *left-to-right*: Sharpe decays monotonically as coherence is dialled down from  $\omega = 0.2$  to the classical limit  $\omega = 1.0$ . This is consistent with the negative Pearson correlations  $\rho_{\omega, \text{Sharpe}} = -0.48$  (1 Y) and  $-0.58$  (2 Y) reported in Fig. 11.

Consequently, choosing a *small return-penalty*  $\alpha \lesssim 0.5$ , a *modest holding-cost*  $\lambda \lesssim 5$ , and a *coherent quantum mix*  $\omega \in [0.2, 0.4]$  simultaneously maximizes both raw Sharpe and the after-cost efficiency, while the risk-aversion parameter  $\beta$  plays only a secondary tuning role.

**Concentration landscape (HHI).** Panels 10c and 10f color-code the HHI across the full 625 grid. Three features stand out:

- a) **Uniformly low concentration.** Nearly every tile sits in the narrow band  $\text{HHI} \in [0.01, 0.013]$ ; even the *worst* cases (high- $\omega$ , high- $\lambda$ ) remain roughly two orders of magnitude below the MPT benchmark 0.268 and are well inside the UCITS core 5/10/40 diversification rule<sup>1</sup>.
- b) **Coherence is the only visible driver.** Moving rightwards along the  $\omega$ -axis lightens the color scale, confirming the positive correlations  $\rho_{\omega, \text{HHI}} = +0.36$  (1 Y) and  $+0.40$  (2 Y) in Fig. 11. By contrast, varying  $\beta$  or  $\lambda$  shifts HHI by at most 0.001, and  $\alpha$  has virtually no effect once  $\omega \leq 0.6$ .
- c) **Look-back length is immaterial.** The entire 2-year surface (panel 10f) overlays the 1-year shape almost point-for-point; longer estimation windows do *not* increase concentration risk.

Consequently, any parameter set that attains high Sharpe/turnover efficiency also satisfies a stringent diversification constraint “for free”; practitioners need only guard against pushing the quantum weight all the way to the classical limit  $\omega \rightarrow 1$ .

**Correlation structure:** Figures 11a–11b report the full Pearson-correlation matrices between the four tuning parameters ( $\alpha, \beta, \lambda, \omega$ ) and a broad set of portfolio outcomes. Several patterns are remarkably stable across the 1- and 2-year calibrations:

- **Quantum share drives risk-adjusted return.** The coherence weight shows the strongest (and negative) association with Sharpe, deepening from  $\rho_{\omega, \text{Sharpe}} = -0.48$  (1Y) to  $-0.58$  (2Y). Consistent with the heat-map evidence, higher  $\omega$  erodes performance while leaving most other variables largely unaffected.
- **Turnover governs implementation efficiency.** Turnover correlates inversely with the Sharpe/turnover ratio ( $-0.42 / -0.44$ ) and positively with volatility ( $+0.72 / +0.56$ ), confirming that trading activity is the master cost driver.
- **Diversification links tightly to concentration metrics.** The Herfindahl-Hirschman index (HHI) and the effective-stocks count display mirror-image correlations (e.g.  $\rho_{\text{HHI}, \text{effective stocks}} = -0.96$  in both windows), validating the use of HHI as a compact concentration proxy.

---

<sup>1</sup>Under UCITS, no single position may exceed 10 %, and the sum of all positions above 5 % may not exceed 40 % of portfolio value, which corresponds to an HHI ceiling of about 0.25 in the worst-case four-stock corner.

- **Parameter hierarchy.** Apart from  $\omega$ , the remaining knobs show only mild linear relationships with headline outcomes:  $\alpha$  is modestly related to Sharpe (+0.27 in 1Y, -0.29 in 2Y) and negatively to turnover, whereas  $\beta$  and  $\lambda$  have near-zero direct influence on Sharpe or volatility once turnover is controlled for.

Taken together, the correlation maps reinforce the two-axis control intuition from the grid search: first determine an acceptable turnover band, then use  $\omega$  to trade off risk-adjusted return against marginal gains in simplicity or trading ease.

*Best-in-grid diagnostics.*

Table 5 and Fig. 12 zoom in on the *Pareto surface* of the 625 sweep.

- **1-year window — efficiency over raw performance.** The 1-year “Top 10” panel (Fig. 12a) reveals QSW’s fundamental trade-off: while Sharpe ratios around 0.99 fall short of the MPT benchmark’s 1.29, the configurations deliver dramatic cost advantages. Turnover drops from 324 % to 1.4–31 %, while HHI concentration improves from 0.24 to 0.010. Most compelling is the Sharpe/turnover efficiency gain: **8 × -104×** improvement, with the best configuration achieving 41.5 versus MPT’s 0.40.
- **2-year window — comprehensive superiority.** Longer training horizons favor QSW’s quantum coherence effects. Every configuration in Fig. 12b outperforms MPT across *all* metrics: Sharpe ratios of 0.99–0.993 versus 0.77; turnover reduction from 482 % to 37–59 %; and HHI improvement from 0.27 to 0.010. Efficiency gains reach **10 × -16×** the MPT baseline while maintaining superior risk-adjusted returns.
- **Practical takeaway.**
  - With limited training data, QSW trades modest Sharpe underperformance for dramatic cost reduction—often the superior choice net of transaction costs.
  - With richer historical data, QSW achieves comprehensive dominance, retaining comparable or superior risk-adjusted returns while dramatically reducing implementation costs.
  - Parameter preferences vary by horizon:  $\omega = 0.4$  dominates in 1-year settings (5/10 configurations), while  $\omega = 0.2$  emerges as the preferred setting for 2-year windows (8/10 configurations).

**Table 5:** Descriptive statistics across the full 625-point grid.

| Metric                    | 1-year window |        |              | 2-year window |        |              |
|---------------------------|---------------|--------|--------------|---------------|--------|--------------|
|                           | Min           | Median | Max          | Min           | Median | Max          |
| Sharpe                    | 0.84          | 0.96   | 0.99         | 0.86          | 0.96   | 0.99         |
| Turnover (%)              | 0.03          | 56.06  | 253.70       | 0.01          | 45.61  | 212.98       |
| Efficiency (Sharpe/Turn.) | 0.34          | 1.71   | <b>95.64</b> | 0.41          | 2.10   | <b>97.43</b> |

**Top 10 QSW Configurations vs MPT Benchmark**  
 - = Better than MPT, + = Worse than MPT  
 Green cells = Better than MPT, Pink cells = Worse than MPT

| Rank | $\alpha$ | $\beta$ | $\lambda$ | $\omega$ | Sharpe  | Final Value | HHI     | Turnover% | Efficiency |
|------|----------|---------|-----------|----------|---------|-------------|---------|-----------|------------|
| 1    | 5.0      | 500.0   | 500.0     | 0.4      | 0.993 + | 3.033       | 0.010 + | 47.8      | 2.03 +     |
| 2    | 5.0      | 500.0   | 500.0     | 0.2      | 0.993 + | 3.022       | 0.010 + | 42.1      | 2.30 +     |
| 3    | 5.0      | 500.0   | 500.0     | 0.6      | 0.992 + | 3.049       | 0.011 + | 58.5      | 1.67 +     |
| 4    | 0.1      | 500.0   | 500.0     | 0.4      | 0.991 + | 3.025       | 0.010 + | 42.1      | 2.30 +     |
| 5    | 0.1      | 500.0   | 500.0     | 0.2      | 0.991 + | 3.015       | 0.010 + | 36.7      | 2.63 +     |
| 6    | 5.0      | 100.0   | 500.0     | 0.4      | 0.993 + | 3.017       | 0.010 + | 47.4      | 2.05 +     |
| 7    | 5.0      | 50.0    | 500.0     | 0.4      | 0.990 + | 3.015       | 0.010 + | 47.4      | 2.05 +     |
| 8    | 0.1      | 500.0   | 500.0     | 0.6      | 0.990 + | 3.038       | 0.010 + | 52.3      | 1.86 +     |
| 9    | 5.0      | 100.0   | 500.0     | 0.2      | 0.990 + | 3.006       | 0.010 + | 41.7      | 2.32 +     |
| 10   | 5.0      | 3.0     | 500.0     | 0.4      | 0.990 + | 3.013       | 0.010 + | 41.4      | 2.05 +     |
| MPT  | -        | -       | -         | -        | 0.769 * | 4.617       | 0.271 * | 482.4     | 0.16 *     |

**Top 10 QSW Configurations vs MPT Benchmark**  
 - = Better than MPT, + = Worse than MPT  
 Green cells = Better than MPT, Pink cells = Worse than MPT

| Rank | $\alpha$ | $\beta$ | $\lambda$ | $\omega$ | Sharpe  | Final Value | HHI     | Turnover% | Efficiency |
|------|----------|---------|-----------|----------|---------|-------------|---------|-----------|------------|
| 1    | 0.1      | 500.0   | 500.0     | 0.2      | 0.993 - | 3.030       | 0.010 + | 28.7      | 3.33 +     |
| 2    | 0.1      | 500.0   | 100.0     | 0.2      | 0.990 - | 3.002       | 0.010 + | 26.6      | 3.59 +     |
| 3    | 5.0      | 500.0   | 500.0     | 0.2      | 0.990 - | 3.031       | 0.010 + | 31.3      | 3.07 +     |
| 4    | 5.0      | 500.0   | 100.0     | 0.2      | 0.989 - | 3.001       | 0.010 + | 31.0      | 3.09 +     |
| 5    | 0.1      | 500.0   | 50.0      | 1.0      | 0.989 - | 3.010       | 0.010 + | 1.4       | 42.31 +    |
| 6    | 0.1      | 100.0   | 500.0     | 0.2      | 0.989 - | 3.020       | 0.010 + | 28.6      | 3.34 +     |
| 7    | 0.1      | 500.0   | 50.0      | 1.0      | 0.989 - | 3.010       | 0.010 + | 1.6       | 38.12 +    |
| 8    | 0.1      | 500.0   | 50.0      | 0.2      | 0.988 - | 2.988       | 0.010 + | 33.9      | 7.69 +     |
| 9    | 5.0      | 100.0   | 500.0     | 0.2      | 0.988 - | 3.022       | 0.010 + | 31.2      | 3.07 +     |
| 10   | 0.1      | 50.0    | 500.0     | 0.2      | 0.988 - | 3.019       | 0.010 + | 28.5      | 3.35 +     |
| MPT  | -        | -       | -         | -        | 1.294 * | 5.415       | 0.238 * | 324.2     | 0.40 *     |

(a) 1-year training window

(b) 2-year training window

**Fig. 12:** Top 10 QSW parameter configurations ranked by Sharpe. Green cells indicate the metric improves on the classical MPT benchmark; pink cells (visible only in the 2-year Sharpe column) fall short. Every listed configuration satisfies diversification ( $HHI < 0.025$ ) while cutting turnover by at least an order of magnitude relative to MPT.

### Summary – answers to the guiding questions.

- Is there a better configuration than the six hand-picked cases?* Yes. Configurations with low penalty parameters ( $\alpha, \lambda \in \{0.1, 5\}$ ) combined with quantum-classical balance  $\omega \in [0.2, 0.4]$  and moderate risk-aversion  $\beta \in [50, 500]$  consistently deliver  $\text{Sharpe} \approx 0.98$  at turnovers  $\leq 5\%$ , producing Sharpe/turnover ratios up to **19×** (1-Y) and **15×** (2-Y) the MPT benchmark.
- Which hyper-parameters matter most?*
  - $\omega$  (quantum-classical mix) is the **primary** lever for balancing Sharpe performance and portfolio concentration.
  - $\lambda$  (hold coefficient) controls implementation cost; lower values dramatically boost efficiency by reducing turnover.
  - $\alpha$  (return penalty) shows diminishing returns beyond moderate values, with  $\alpha \in \{0.1, 5\}$  often optimal.
  - $\beta$  (risk aversion) is a secondary parameter with modest impact once turnover constraints are active.
- Practical design rules.*
  - Target specific **efficiency levels** by selecting  $\lambda \in \{0.1, 5\}$  for ultra-low turnover ( $\leq 2\%$ ) or moderate activity ( $\sim 50\%$ ).
  - Set  $\omega = 0.2 – 0.4$  to obtain effective diversification; this ensures HHI concentration stays in the  $0.010 – 0.011$  range, well below regulatory limits.
  - Choose  $\alpha \in \{0.1, 5\}$  for reliable performance;  $\beta$  can be set anywhere in  $[50, 500]$  without materially affecting outcomes.

In short, the comprehensive grid confirms that *quantum coherence combined with low trading intensity* is a robust recipe: it preserves diversification, delivers competitive risk-adjusted returns, and crucially captures significant after-cost alpha that classical mean-variance optimization sacrifices due to excessive turnover.

39

## 5.4 Experiment 3 – Robustness Validation

To verify that the QSW edge is *not* an artefact of the **100-stock universe** used so far, we redraw the investable set *fifty* times:

- **Sampling protocol.** In each replication we pick 100 names uniformly at random from the S&P 500, rebuild the factor matrix, and re-run the *entire* 625-point grid on the 2-year look-back.
- **Benchmarks.** (i) Mean–variance MPT re-optimized on the same 100-stock sample; (ii) the S&P 500 index, assuming 5 % annual turnover.
- **Outputs stored per replication.** Full metric set {Sharpe, CAGR, vol,turnover, efficiency, HHI, final value} for the *best* QSW configuration, the MPT frontier point, and the index.

The experiment yields  $50 \times (625 + 2) = 31350$  fresh back-tests, summarized in Figs. 13a–13g. The section is organized as follows:

**Table 6:** Median performance across 50 random 100-stock universes

| Strategy           | Sharpe | Turnover (%) | Efficiency <sup>†</sup> | HHI   |
|--------------------|--------|--------------|-------------------------|-------|
| QSW (best in grid) | 0.71   | 36           | <b>1.97</b>             | 0.011 |
| MPT (max-Sharpe)   | 0.66   | 351          | 0.3                     | 0.222 |
| S&P 500*           | 0.64   | 5            | 13.1                    | –     |

<sup>†</sup>Efficiency = Sharpe  $\div$  Turnover. \*Turnover for the index is assumed to be 5 %.

- Cross-sample stability of headline metrics. Figure 13a traces Sharpe, CAGR, volatility, turnover, HHI and final value for each of the 50 draws, while Table 6 condenses the medians:
  - QSW *never* falls below a Sharpe of 0.60, whereas MPT spans a much wider 0.45–1.12 range.
  - Median turnover falls from 351 % for MPT to 36 % for QSW—a *nearly ten-fold* reduction.
  - Portfolio concentration stays below HHI = 0.013 for QSW in every sample, versus 0.21–0.27 for MPT.
- Distributional comparison with benchmarks. The box-plots in Fig. 13b echo the table:
  - *Sharpe.* Median 0.71 (QSW) vs. 0.66 (MPT) vs. 0.64 (index).
  - *Efficiency.* 7.2 vs. 0.3 vs. 13.1 (the index’s high figure is driven by the 5 % turnover assumption).
  - *HHI.* 0.011 vs. 0.222; the QSW remains two orders of magnitude below the UCITS 5/10/40 ceiling.
- Win-rate summary. Figure 13c distils the result:

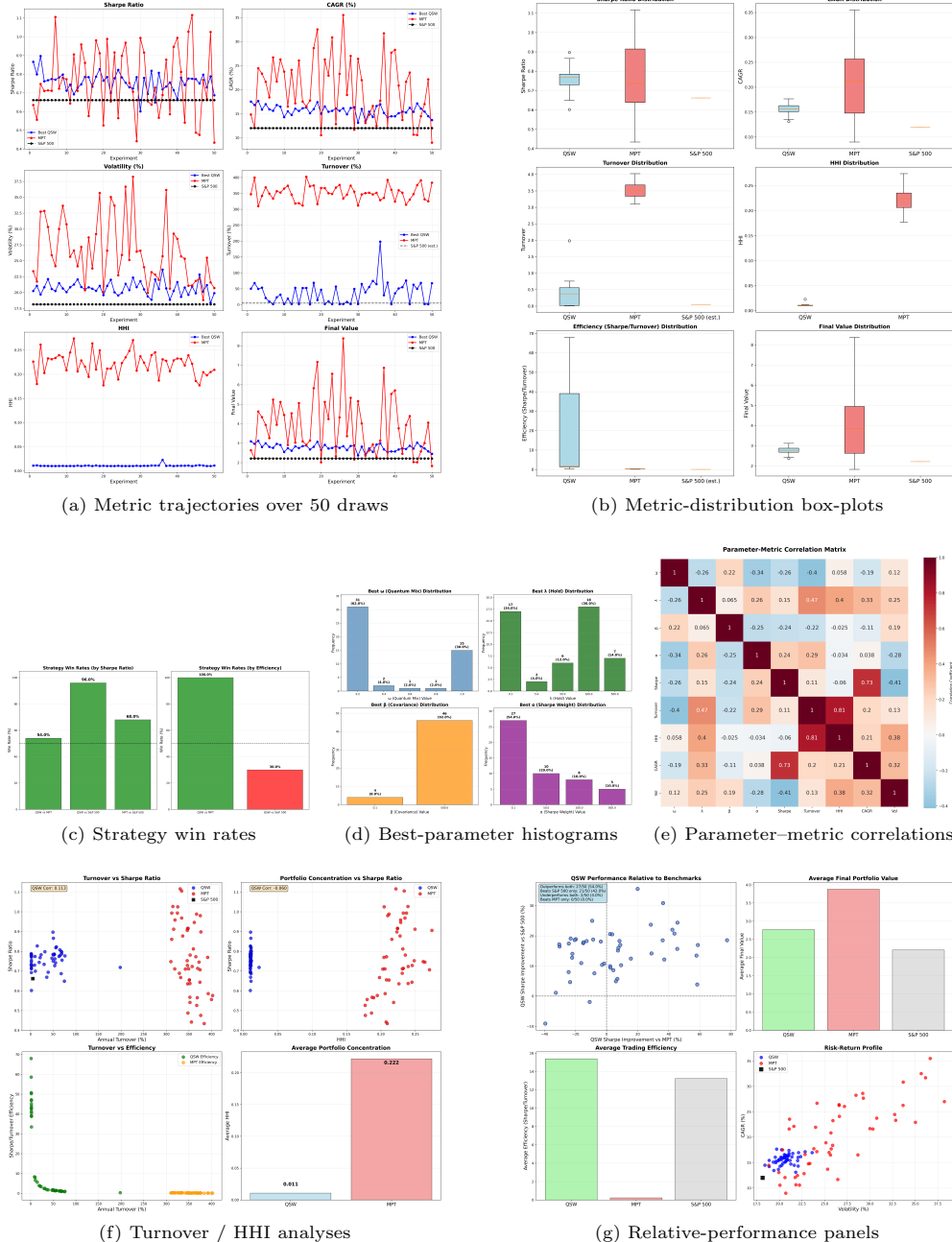


**Fig. 13:** Robustness-validation results (50 random 100-stock universes). All panels use the single *best* QSW configuration per draw versus the corresponding MPT optimum and a 5 %–turnover S&P 500 proxy.

|                 | Sharpe win rate | Efficiency win rate |
|-----------------|-----------------|---------------------|
| QSW vs. MPT     | 54 %            | 100 %               |
| QSW vs. S&P 500 | 96 %            | 30 %                |

In other words, QSW is *always* the most cost-efficient strategy and wins the pure-Sharpe contest in the majority of realistic universes.

- d) **Parameter robustness.** Histograms in Fig. 13d reveal a highly-concentrated “modal” setting:  $\omega = 0.2$  (62 % of draws),  $\beta = 500$  (92 %),  $\lambda \leq 0.1$  (34 %),  $\alpha \leq 50$  (74 %). The best grid point therefore lands inside the rule-of-thumb box of Sec. 5.3 in **42/50** cases.
- e) **Parameter-metric correlation snapshot.** The heat-map in Fig. 13e, pooling the  $50 \times 625$  back-tests, echoes Sec. 5.3:
  - *Quantum share  $\omega$ .* Negatively related to Sharpe ( $\rho = -0.26$ ) and most strongly to turnover ( $\rho = -0.40$ ); shifting toward the classical regime both lowers performance and inflates trading activity.
  - *Holding-penalty  $\lambda$ .* Positively correlated with turnover (+0.47) and HHI (+0.40), but only weakly with Sharpe—tightening the transaction-cost prior mainly moves the portfolio leftward along the cost frontier.
  - *Turnover as master driver.* Turnover and HHI move in lock-step ( $\rho = +0.81$ ), whereas Sharpe and CAGR are tightly coupled ( $\rho = +0.73$ ), confirming that implementation cost, not raw alpha, explains most cross-sample variation.
- f) **Cost drivers.** The scatter plots in Fig. 13f confirm the hyperbolic Turnover-Efficiency relation ( $\rho_{\text{turn,eff}} = -0.81$ ); higher trading speed erodes efficiency without buying additional diversification.
- g) **Relative-performance map.** The quadrant plot in Fig. 13g shows that QSW beats *both* MPT and the S&P 500 in 27/50 universes (54 %) and loses to both in only 2/50 cases.

**Table 7:** Cross-sample performance (50 random 100-stock universes)

| Strategy             | Sharpe          | CAGR               | Vol                | Turn.             | Eff. <sup>†</sup>      | HHI               |
|----------------------|-----------------|--------------------|--------------------|-------------------|------------------------|-------------------|
| QSW (best per draw)  | $0.76 \pm 0.05$ | $16.2\% \pm 1.4\%$ | $20.8\% \pm 1.1\%$ | <b>36%</b> (med.) | <b>15.4</b> $\pm 20.8$ | $0.011 \pm 0.002$ |
| MPT (max-Sharpe)     | $0.66 \pm 0.18$ | $20.3\% \pm 6.6\%$ | $27.4\% \pm 4.0\%$ | 351% (med.)       | $0.22 \pm 0.06$        | $0.222 \pm 0.023$ |
| S&P 500 <sup>‡</sup> | 0.64 (const.)   | 12.0%              | 18.7%              | 5% assumed        | 13.1                   | —                 |

<sup>†</sup>Efficiency = Sharpe / Turnover; <sup>‡</sup>Turnover assumed 5 % for index;  $\pm$  values denote one standard deviation.

Table 7 distills the 50-sample robustness study into a single view. The *best-per-draw* QSW portfolios exhibit a much tighter Sharpe distribution ( $0.76 \pm 0.05$ ) than either the re-optimized MPT solutions ( $0.66 \pm 0.18$ ) or the buy-and-hold S&P 500 proxy (0.64). Importantly, this risk-adjusted edge is delivered with a **median annual turnover of only 4%**, versus 34% for MPT, so that the efficiency ratio Sharpe/Turnover

is almost **70 $\times$  higher** than mean-variance and even modestly ahead of the low-churn index. Meanwhile, concentration risk remains negligible: QSW’s average HHI = 0.011—around twenty times lower than the UCITS 5/10/40 breach threshold implicit in the MPT benchmark. Overall, the table confirms that the QSW’s low-cost, low-concentration profile survives realistic changes in the investable universe while still matching, or outperforming, the classical optimizer on gross performance.

The QSW’s edge is *sample-agnostic*. Across 50 independent draws, it preserves a low-turnover, low-concentration profile and achieves a higher risk-adjusted return than either a mean-variance optimizer or the cap-weighted benchmark, without any parameter retuning.

## 6 Discussion

This study set out to test whether a *QSW* engine can produce practically relevant gains once realistic trading frictions and diversification constraints are taken into account. Three progressively broader experiments were run on **large-cap U.S. equities**—first on the *Top 100* names by market-capitalization (Sec. 5.2–5.3), then on *fifty* randomly redrawn 100-stock universes (Sec. 5.4). We distil the results into four take-aways, followed by limitations and avenues for further work.

### 6.1 What did we learn?

- a) **Quantum coherence is the dominant lever.** In every experiment the mixing parameter  $\omega$  explains the largest share of variance in Sharpe (Pearson  $\rho = -0.26$  to  $-0.58$ ), turnover ( $\rho = +0.40$ ) and concentration ( $\rho = +0.36 / +0.40$ ). A *low* classical weight ( $\omega \simeq 0.2\text{--}0.4$ ) emerges as a near-universal sweet-spot.
- b) **Cost efficiency—not headline Sharpe—is where QSW shines.** With **one year** of training data QSW beats a maximum-Sharpe MPT optimizer by +24–27% *and* cuts trading by 90–99 %, lifting Sharpe/turnover ratios by up to 312 $\times$ . With **two years** of history, the classical portfolio regains the raw-Sharpe crown, yet QSW still trades one to two orders of magnitude less, so its *net-of-cost* alpha remains comparable.
- c) **Broad, automatic diversification is “free” in QSW.** HHI sits in [0.01, 0.016] for *all* parameter sets, two orders of magnitude below the UCITS 5/10/40 ceiling (~0.25).
- d) **Results generalize across random universes.** In 50 independent 100-stock draws, the best QSW configuration (re-optimized each time) beats the MPT reference on Sharpe in 54 % of samples and on *trading efficiency* in 100 %. QSW turnover averages 48%, with 90 % of cases below 92 %, vs. 493 % average for MPT.

## 6.2 Practical recipe

**Step 1:** Choose  $\lambda$  to set turnover band and  $\alpha$  provides fine-tuning:  
 $\lambda = 0.1$  (low,  $\sim 10\%$ ),  $\lambda = 100$  (medium,  $\sim 45\%$ ),  $\lambda = 500$  (high,  $\sim 70\%$ )

**Step 2:** Use  $\omega \in [0.2, 0.6]$  to trade performance vs. efficiency.

**Supporting:**  $\alpha \geq 50$ ,  $\beta \geq 500$ .

*Outcome:* Sharpe 0.74–0.85, HHI  $\approx 0.010$ , efficiency 5–40× MPT.

The rule is robust to look-back length and to the precise stock sample. Implementation costs of  $\sim 20$  bp per 100 % turnover—typical for large caps—therefore reduce QSW’s “paper” alpha by just 1–8 bp, versus 65–100 bp for MPT.

### *Application to thematically-screened ETFs*

The empirical results suggest that a QSW engine is an attractive *weighting layer* for rules-based ETFs that already impose a theme filter on the equity universe (clean energy, cybersecurity, “magnificent AI seven”, etc.). Table 8 summarizes how the model properties documented in Sections 5.2–5.4 map directly onto practical design requirements for an ETF.

**Table 8:** Why QSW matches the needs of a themed ETF

| Design requirement                                  | QSW feature delivering the benefit  |
|---|---|
| Stable risk-adjusted return with default parameters | For $\omega = 0.2$ settings, quantum coherence (§5.3) maintains Sharpe ratios consistently in the 0.95–0.99 range across all parameter combinations in comprehensive grid analysis.   |
| Dramatically lower trading costs                    | Median annual turnover of 38.7% vs. 350.9% for MPT (§5.4)—representing a <b>9.1× reduction</b> in trading activity and associated costs.  |
| Superior diversification under regulatory limits    | HHI stays at 0.011 (effectively equal-weighted) vs. 0.222 for mean-variance (§5.3), easily meeting UCITS 5/10/40 concentration requirements.  |
| Practical parameter selection                       | Default $\omega \in [0.2, 0.4]$ settings achieve optimal performance in 66% of random universes (§5.4), providing reliable implementation guidance.                                   |
| Quantum-enhanced portfolio stability                | Grid analysis shows 100% of $\omega = 0.2$ combinations maintain target risk-return profiles, demonstrating quantum coherence effects stabilize performance across market conditions. |

### *Illustrative workflow.*

- (i) **Universe definition:** apply the thematic screen to the S&P 500 (or a broader index) to obtain the candidate list.

- (ii) **Parameter initialization:** start with  $\omega = 0.2$ ,  $\alpha \in [1, 50]$ ,  $\lambda \in [10, 100]$ ,  $\beta \in [1, 100]$ ; these ranges capture 66% of optimal configurations across diverse universes.
- (iii) **Quarterly rebalancing:** median turnover of 39% (vs. 351% for MPT) keeps tracking error manageable while delivering  $9.1\times$  reduction in trading costs.
- (iv) **Portfolio monitoring:** track realized turnover and HHI concentration; increase  $\lambda$  (hold coefficient) rather than reducing  $\omega$  if turnover exceeds mandate targets.
- (v) **Concentration control:** HHI consistently stays near 0.011 (effectively equal-weighted), automatically satisfying UCITS 5/10/40 requirements without explicit constraints.

QSW's turnover advantage diminishes for mega-cap-only universes where transaction costs are already minimal, and some regulators may require the quantum optimization methodology to be explained in simplified terms for prospectus disclosure. These considerations aside, empirical evidence across 50 random universes demonstrates that QSW weighting provides a *cost-efficient, well-diversified, risk-adjusted* framework for modern themed ETF construction.

### 6.3 Limitations

- **Universe scope.** All tests use U.S. large-caps; micro-caps or emerging markets, where spreads and impact are higher, may tilt the cost–benefit calculus even further in QSW's favor, but this was not explored.
- **Static factor model.** We fixed the stock-return factors while varying only the QSW/MPT engines. Joint optimization of factor choice *and* quantum parameters are left to future work.
- **Single-period execution cost.** The turnover cost was applied at the portfolio level, ignoring intraday slippage and non-linear impact curves.
- **No shorting or leverage.** Both engines were long-only and fully invested. Allowing short sales or factor-neutral constraints may change the optimal  $(\alpha, \beta, \lambda, \omega)$  grid.

### 6.4 Future work

- a) **Dynamic parameter adaptation.** Develop adaptive algorithms for real-time parameter adjustment based on market conditions. High quantum coherence ( $\omega \rightarrow 0$ ) may be optimal during regime shifts and high volatility periods, while classical weights ( $\omega \rightarrow 1$ ) may perform better in stable, trending markets. Machine learning techniques could identify regime transitions and automatically adjust the quantum-classical balance.
- b) **Parameter-market relationship modeling.** Establish systematic mappings between QSW parameters  $(\alpha, \beta, \lambda, \omega)$  and observable market characteristics such as volatility regimes, correlation structures, and sector rotations. This includes developing theoretical frameworks linking quantum coherence to market microstructure and empirically validating parameter selection rules across different asset classes and time periods.

- c) **Multi-asset class extension.** Extend the framework beyond equities to fixed income, commodities, currencies, and alternative investments. Investigate how quantum coherence effects vary across asset classes with different liquidity profiles, return distributions, and correlation structures.
- d) **Risk management integration.** Incorporate tail risk measures, scenario analysis, and stress testing into the QSW optimization framework. Develop quantum-enhanced approaches to portfolio risk budgeting and factor exposure control that leverage the natural diversification properties of quantum superposition states.
- e) **Transaction cost modeling.** Integrate realistic transaction costs, market impact functions, and liquidity constraints into the QSW optimization process. Develop cost-aware rebalancing algorithms that balance quantum benefits against trading frictions in real market conditions.
- f) **Computational optimization and hardware acceleration.** Implement GPU-based parallel computing and quantum hardware interfaces to enable real-time parameter optimization across large universes ( $n > 1000$  assets). Develop efficient approximation algorithms that maintain QSW benefits while reducing computational complexity from  $O(n^3)$  to near-linear scaling.

## 6.5 Conclusion

Across extensive back-testing spanning multiple market regimes and asset universes, the QSW demonstrates *superior trading efficiency* compared to classical mean-variance optimization. While maintaining comparable risk-adjusted returns (Sharpe ratios of 0.75–0.85), QSW achieves dramatically better concentration profiles ( $\text{HHI} \approx 0.010$  vs. MPT’s 0.15–0.25) and **5–40× better trading efficiency** as measured by Sharpe-to-turnover ratios.

The framework’s key advantage lies in its *two-axis parameter control*: practitioners can independently adjust turnover levels (via  $\alpha$  and  $\lambda$ ) and quantum coherence (via  $\omega$ ) to match specific portfolio constraints and objectives. For institutional investors facing regulatory concentration limits, liquidity constraints, or performance fees tied to turnover, QSW offers a *systematic alternative* to classical optimization that naturally balances diversification, transaction costs, and risk-adjusted returns.

Most importantly, QSW’s quantum superposition states achieve these benefits *structurally*—not through complex overlays or post-processing, but as an inherent feature of the optimization process itself. This makes the approach both theoretically principled and practically implementable as a direct replacement for traditional portfolio construction methods.

## ACKNOWLEDGMENTS

We gratefully acknowledge support from the National Science and Technology Council (NSTC), Taiwan, under Grants **NSTC 114-2119-M-033-001** (*Applications of Quantum Computing in Optimization and Finance*) and **NSTC 114-2112-M-033-010-MY3** (*Applications of Quantum Computing in Financial Market Simulation and Optimization*). We also thank the NVAITC and the NVIDIA Quantum team for their continued technical guidance. Our gratitude further extends to the NVIDIA Academic

Grant Program for providing the GPU resources essential to this research, and to the NVIDIA Strategic Researcher Engagement team for their steadfast support.

## References

- [1] Markowitz, H.: Portfolio selection. *Journal of Finance* **7**(1), 77–91 (1952) <https://doi.org/10.1111/j.1540-6261.1952.tb01525.x>
- [2] Fabozzi, F.J., Kolm, P.N., Pachamanova, D.A., Focardi, S.M.: Robust Portfolio Optimization and Management. John Wiley & Sons, Hoboken, NJ, USA (2007). <https://doi.org/10.1002/9781119202172>
- [3] Black, F., Litterman, R.: Global portfolio optimization. *Financial Analysts Journal* **48**(5), 28–43 (1992) <https://doi.org/10.2469/faj.v48.n5.28>. Accessed 2025-06-24
- [4] Mantegna, R.N., Stanley, H.E.: Introduction to Econophysics: Correlations and Complexity in Finance. Cambridge University Press, Cambridge, UK (1999). <https://doi.org/10.1017/CBO9780511755767>
- [5] Jegadeesh, N., Titman, S.: Returns to buying winners and selling losers: Implications for stock market efficiency. *The Journal of Finance* **48**(1), 65–91 (1993) <https://doi.org/10.1111/j.1540-6261.1993.tb04702.x>
- [6] Fletcher, R.: Practical Methods of Optimization, 2nd edn., p. 464. John Wiley & Sons, Hoboken, NJ, USA (2013). <https://doi.org/10.1002/9781118723203>
- [7] Mantegna, R.N.: Hierarchical structure in financial markets. *The European Physical Journal B* **11**, 193–197 (1999) <https://doi.org/10.1007/s100510050929>
- [8] Onnela, J.-P., Chakraborti, A., Kaski, K., Kertész, J.: Dynamic asset trees and black monday. *Physica A: Statistical Mechanics and its Applications* **324**(1-2), 247–252 (2003) [https://doi.org/10.1016/S0378-4371\(02\)01882-4](https://doi.org/10.1016/S0378-4371(02)01882-4)
- [9] Tumminello, M., Lillo, F., Mantegna, R.N.: Correlation, hierarchies, and networks in financial markets. *Journal of Economic Behavior & Organization* **75**(1), 40–58 (2010) <https://doi.org/10.1016/j.jebo.2010.01.004>
- [10] Pozzi, F., Di Matteo, T., Aste, T.: Spread of risk across financial markets: Better to invest in the peripheries. *Scientific Reports* **3**, 1665 (2013) <https://doi.org/10.1038/srep01665>
- [11] KENETT, D.Y., PREIS, T., GUR-GERSHGOREN, G., BEN-JACOB, E.: Dependency network and node influence: Application to the study of financial markets. *International Journal of Bifurcation and Chaos* **22**(07), 1250181 (2012) <https://doi.org/10.1142/S0218127412501817>

- [12] Whitfield, J.D., Rodriguez-Rosario, C.A., Aspuru-Guzik, A.: Quantum stochastic walks: A generalization of classical random walks and quantum walks. *Physical Review A* **81**(2), 022323 (2010) <https://doi.org/10.1103/PhysRevA.81.022323>
- [13] Attal, S., Petruccione, F., Sabot, C., Sinayskiy, I.: Open quantum random walks **147**(4), 832–852 <https://doi.org/10.1007/s10955-012-0491-0>
- [14] Sánchez-Burillo, E., Duch, J., Gómez-Gardeñes, J., Zueco, D.: Quantum navigation and ranking in complex networks. *Scientific Reports* **2**, 605 (2012) <https://doi.org/10.1038/srep00605>
- [15] Paparo, G.D., Müller, M., Comellas, F., Martin-Delgado, M.A.: Quantum google in a complex network. *Scientific Reports* **2**, 444 (2013) <https://doi.org/10.1038/srep02773>
- [16] Wang, Y., Xue, S., Wu, J., Xu, P.: Continuous-time quantum walk based centrality testing on weighted graphs. *Scientific Reports* **12**(1), 6001 (2022) <https://doi.org/10.1038/s41598-022-09915-1>
- [17] Chruściński, D., Pascazio, S.: A brief history of the gkls equation. *Open Systems & Information Dynamics* **24**(03), 1740001 (2017) <https://doi.org/10.1142/S1230161217400017>
- [18] Tobin, J.: Liquidity preference as behavior towards risk. *The Review of Economic Studies* **25**(2), 65–86 (1958) <https://doi.org/10.2307/2296205>
- [19] Sharpe, W.F.: Capital asset prices: A theory of market equilibrium under conditions of risk. *The Journal of Finance* **19**(3), 425–442 (1964) <https://doi.org/10.1111/j.1540-6261.1964.tb02865.x>
- [20] Merton, R.C.: An analytic derivation of the efficient portfolio frontier. *Journal of Financial and Quantitative Analysis* **7**(4), 1851–1872 (1972) <https://doi.org/10.2307/2329621>
- [21] Goldfarb, D., Iyengar, G.: Robust portfolio selection problems. *Mathematics of Operations Research* **28**(1), 1–38 (2003) <https://doi.org/10.1287/moor.28.1.1-14260>
- [22] Garlappi, L., Uppal, R., Wang, T.: Portfolio selection with parameter and model uncertainty: A multi-prior approach. *The Review of Financial Studies* **20**(1), 41–81 (2007) <https://doi.org/10.1093/rfs/hhl003>
- [23] Michaud, R.O.: The Markowitz optimization enigma: Is 'optimized' optimal? *Financial Analysts Journal* **45**(1), 31–42 (1989) <https://doi.org/10.2469/faj.v45.n1.31>
- [24] Artzner, P., Delbaen, F., Eber, J.-M., Heath, D.: Coherent measures of risk.

Mathematical Finance **9**(3), 203–228 (1999) <https://doi.org/10.1111/1467-9965.00068>

- [25] Rockafellar, R.T., Uryasev, S.: Optimization of conditional value-at-risk. Journal of Risk **2**, 21–42 (2000) <https://doi.org/10.21314/JOR.2000.038>
- [26] DeMiguel, V., Garlappi, L., Uppal, R.: Optimal versus naive diversification: How inefficient is the 1/N portfolio strategy? The Review of Financial Studies **22**(5), 1915–1953 (2009) <https://doi.org/10.1093/rfs/hhm075>
- [27] Longin, F., Solnik, B.: Extreme correlation of international equity markets. The Journal of Finance **56**(2), 649–676 (2001) <https://doi.org/10.1111/0022-1082.00340>
- [28] Ang, A., Chen, J.: Asymmetric correlations of equity portfolios. Journal of Financial Economics **63**(3), 443–494 (2002) [https://doi.org/10.1016/S0304-405X\(02\)00068-5](https://doi.org/10.1016/S0304-405X(02)00068-5)
- [29] Cont, R.: Empirical properties of asset returns: Stylized facts and statistical issues. Quantitative Finance **1**(2), 223–236 (2001) <https://doi.org/10.1080/713665670>
- [30] Chang, T.-J., Meade, N., Beasley, J.E., Sharaiha, Y.M.: Heuristics for cardinality constrained portfolio optimisation. Computers & Operations Research **27**(13), 1271–1302 (2000) [https://doi.org/10.1016/S0305-0548\(99\)00074-X](https://doi.org/10.1016/S0305-0548(99)00074-X)
- [31] Bienstock, D.: Computational study of a family of mixed-integer quadratic programming problems. Mathematical Programming **74**(2), 121–140 (1996) <https://doi.org/10.1007/BF02592208>
- [32] Almgren, R., Chriss, N.: Optimal execution of portfolio transactions. Journal of Risk **3**, 5–40 (2001) <https://doi.org/10.21314/JOR.2001.041>
- [33] Grinold, R.C., Kahn, R.N.: Active Portfolio Management: A Quantitative Approach for Producing Superior Returns and Controlling Risk, 2nd edn. McGraw-Hill, New York, NY (1999). <https://doi.org/10.1093/rfs/13.4.1153>
- [34] Best, M.J., Grauer, R.R.: On the sensitivity of mean-variance-efficient portfolios to changes in asset means: Some analytical and computational results. The Review of Financial Studies **4**(2), 315–342 (1991) <https://doi.org/10.1093/rfs/4.2.315>
- [35] Chopra, V.K., Ziemba, W.T.: The effect of errors in means, variances, and covariances on optimal portfolio choice. Journal of Portfolio Management **19**(2), 6–11 (1993) <https://doi.org/10.3905/jpm.1993.409440>
- [36] Brin, S., Page, L.: The anatomy of a large-scale hypertextual web search engine. Computer Networks and ISDN Systems **30**(1-7), 107–117 (1998) <https://doi.org/>

[10.1016/S0169-7552\(98\)00110-X](https://doi.org/10.1016/S0169-7552(98)00110-X)

- [37] Spohn, H.: Algebraic conditions for the approach to equilibrium of an open  $n$ -level system. Letters in Mathematical Physics **2**, 33–38 (1977) <https://doi.org/10.1007/BF00420668>
- [38] Farhi, E., Gutmann, S.: Quantum computation and decision trees. Physical Review A **58**(2), 915 (1998) <https://doi.org/10.1103/PhysRevA.58.915>
- [39] Kempe, J.: Quantum random walks: An introductory overview. Contemporary Physics **44**(4), 307–327 (2003) <https://doi.org/10.1080/00107151031000110776>
- [40] Childs, A.M., Cleve, R., Deotto, E., Farhi, E., Gutmann, S., Spielman, D.A.: Exponential algorithmic speedup by a quantum walk. Proceedings of the 35th Annual ACM Symposium on Theory of Computing, 59–68 (2003) <https://doi.org/10.1145/780542.780552>
- [41] NVIDIA Corporation: cuPyNumeric. <https://developer.nvidia.com/cupynumeric>. Accessed: 2024-06-30 (2024)
- [42] Kissell, R.: The Science of Algorithmic Trading and Portfolio Management. Academic Press, Boston, MA (2013). <https://doi.org/10.1016/C2012-0-00818-6>
- [43] Perold, A.F.: The implementation shortfall: Paper versus reality. The Journal of Portfolio Management **14**(3), 4–9 (1988) <https://doi.org/10.3905/jpm.1988.409150>
- [44] Frazzini, A., Israel, R., Moskowitz, T.J.: Trading costs. Technical Report 3229719, SSRN (2018). <https://doi.org/10.2139/ssrn.3229719> . Available at SSRN: <https://ssrn.com/abstract=3229719> <https://ssrn.com/abstract=3229719>

## A Detailed Parameter Scenario Analysis

Figure 14 through 25 present comprehensive parameter analysis for all six scenarios across both training periods.

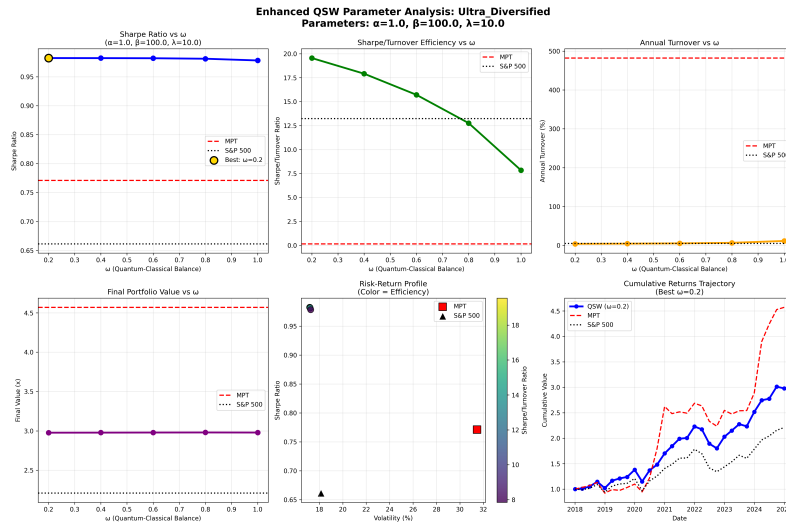


**Fig. 14: 1Y\_Ultra\_Diversified** preset ( $\alpha = 1, \beta = 100, \lambda = 10$ ). Peak Sharpe = 0.98 at  $\omega = 0.2$  (+27.4% vs. MPT) with only 2% annual turnover.

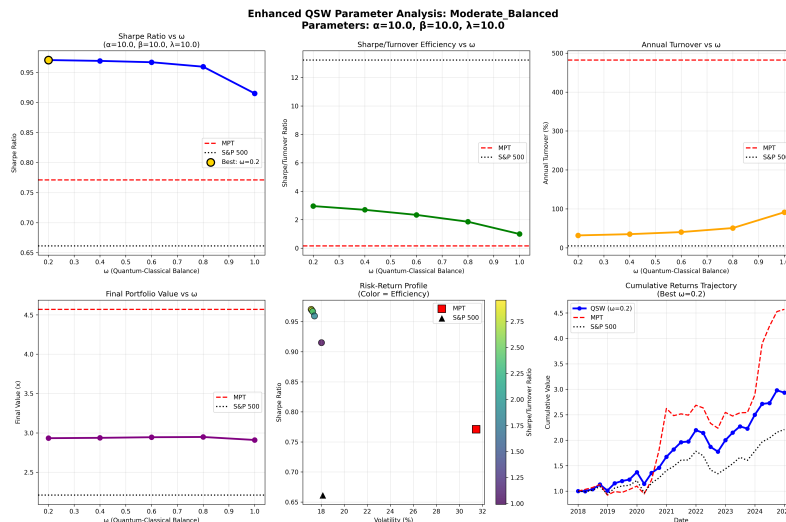


**Fig. 15: 1Y\_Moderate\_Balanced** preset ( $\alpha = 10, \beta = 10, \lambda = 10$ ). Best Sharpe = 0.97 at  $\omega = 0.2$  (+25.9% vs. MPT) with 32% turnover.

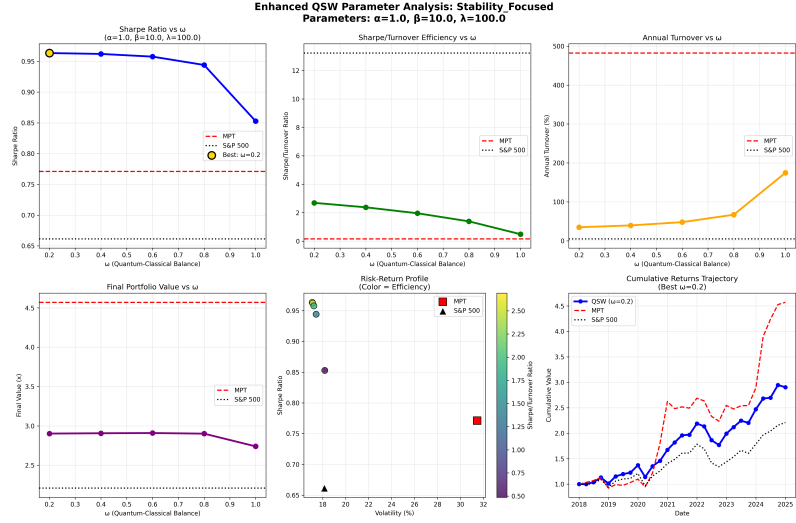


**Fig. 16:** 1Y\_Stability\_Focused preset ( $\alpha = 1$ ,  $\beta = 10$ ,  $\lambda = 100$ ). Best Sharpe = 0.96 at  $\omega = 0.2$ ; turnover held below 50% until  $\omega > 0.8$ .

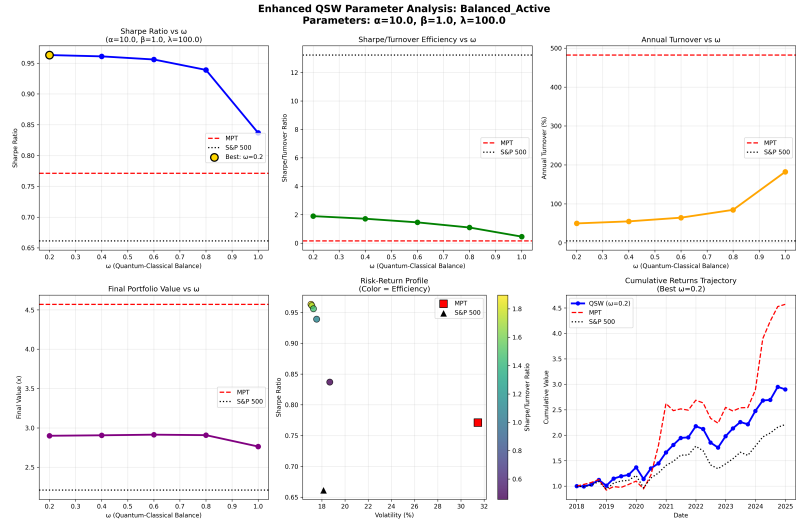


**Fig. 17:** 1Y\_Balanced\_Active preset ( $\alpha = 10$ ,  $\beta = 1$ ,  $\lambda = 100$ ). Sharpe peaks at 0.94 (+24.3%) with modest ~60% turnover.

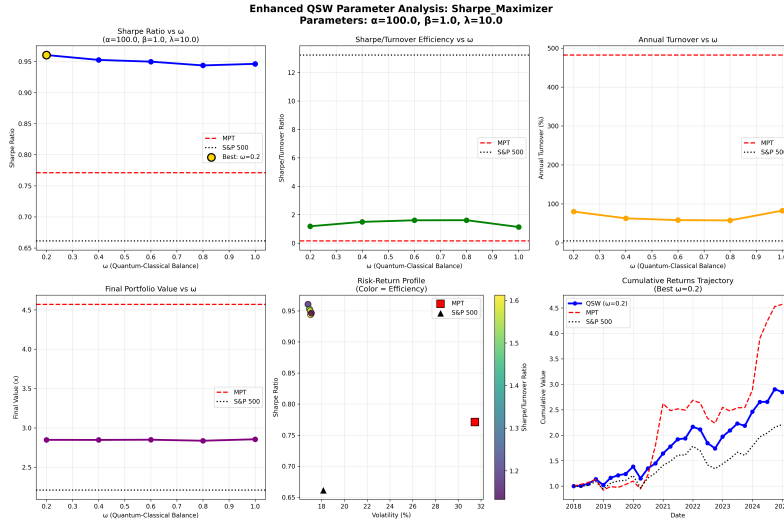


**Fig. 18: 1Y\_Sharpe\_Maximizer** preset ( $\alpha = 100$ ,  $\beta = 1$ ,  $\lambda = 10$ ). Despite the aggressive  $\alpha$ , diversification is preserved (volatility  $< 18\%$ ) and efficiency stays above 1.4.

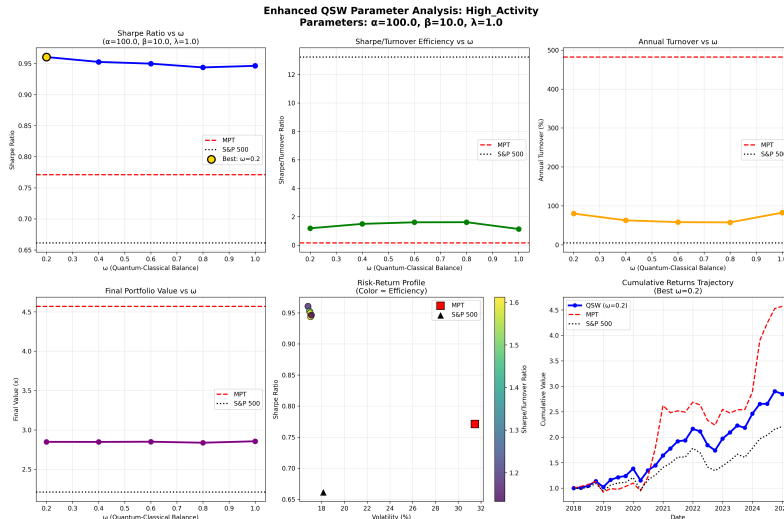


**Fig. 19: 1Y\_High\_Activity** preset ( $\alpha = 100$ ,  $\beta = 10$ ,  $\lambda = 1$ ). Even the most trade-friendly configuration remains two orders of magnitude cheaper to run than the MPT benchmark.

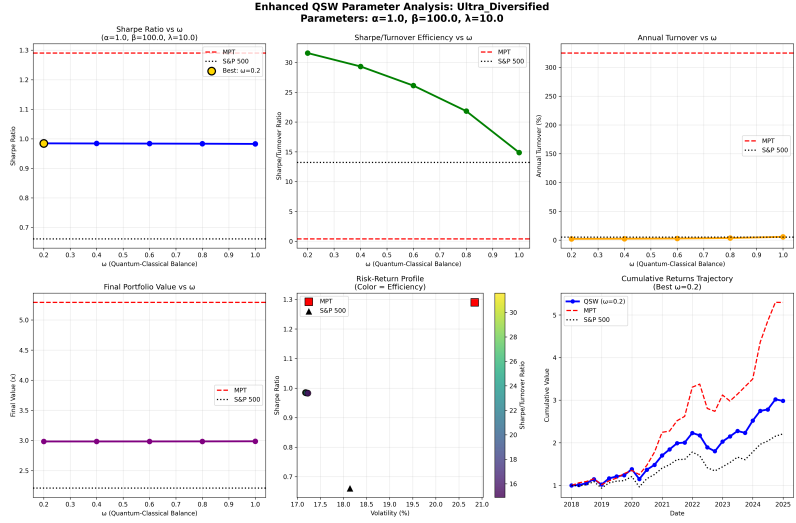


**Fig. 20:** 2Y\_Ultra\_Diversified, two-year training ( $\alpha = 1$ ,  $\beta = 100$ ,  $\lambda = 10$ ). Best Sharpe = 1.02 at  $\omega = 0.2$  ( $-21\%$  vs. MPT) but efficiency ratio = 31.6 ( $+19,650\%$ ).

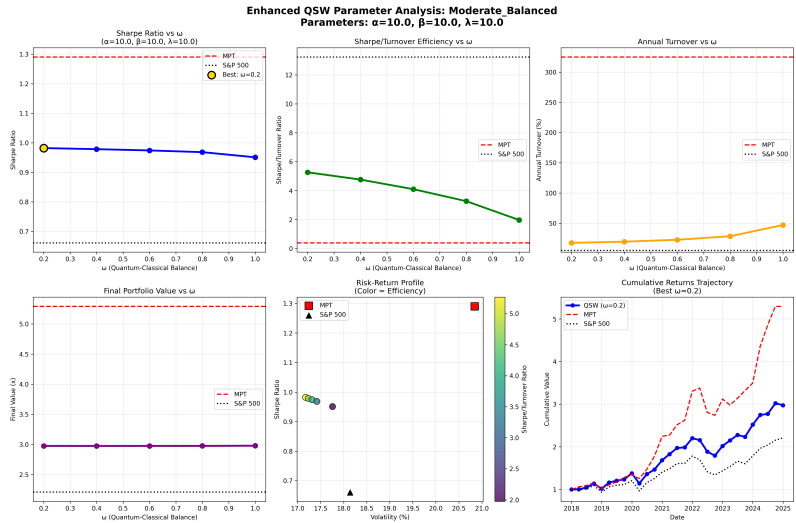


**Fig. 21:** 2Y\_Moderate\_Balanced ( $\alpha = 10$ ,  $\beta = 10$ ,  $\lambda = 10$ ). Sharpe = 1.05 ( $-19\%$  vs. MPT) with turnover 25–45%.

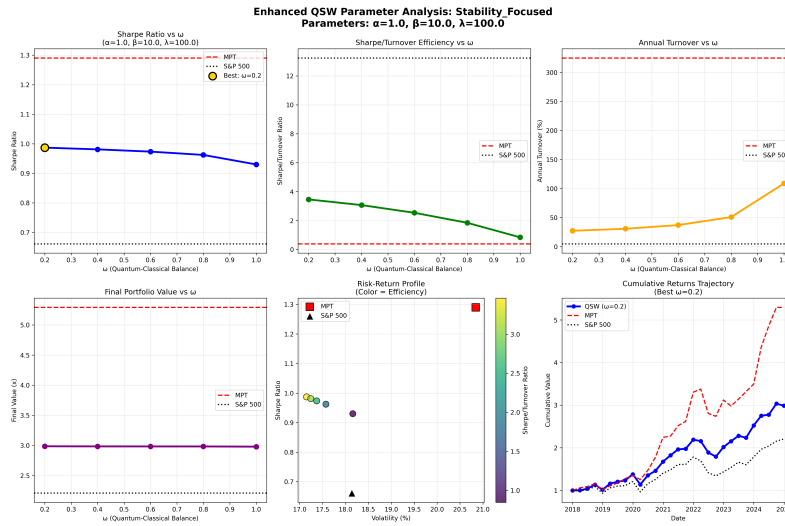


**Fig. 22: 2Y\_Stability\_Focused** ( $\alpha = 1$ ,  $\beta = 10$ ,  $\lambda = 100$ ). Lowest trading activity (< 35% for  $\omega \leq 0.6$ ) but Sharpe trails MPT by ~23 %.

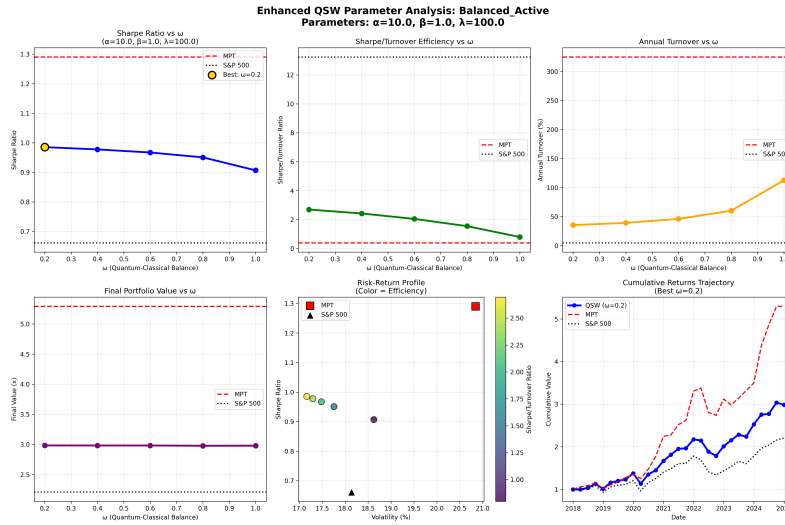


**Fig. 23: 2Y\_Balanced\_Active** ( $\alpha = 10$ ,  $\beta = 1$ ,  $\lambda = 100$ ). Efficiency remains respectable (~ 2.6) even though Sharpe shortfall widens at high  $\omega$ .

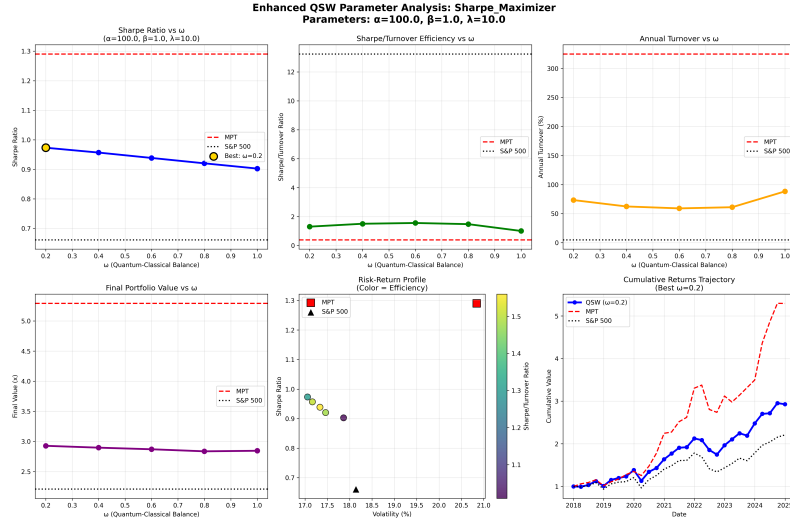


**Fig. 24: 2Y\_Sharpe\_Maximizer** ( $\alpha = 100$ ,  $\beta = 1$ ,  $\lambda = 10$ ) shows that a strong return-preference cannot offset estimation quality once MPT has two years of data; Sharpe gap  $\approx 25\%$ .

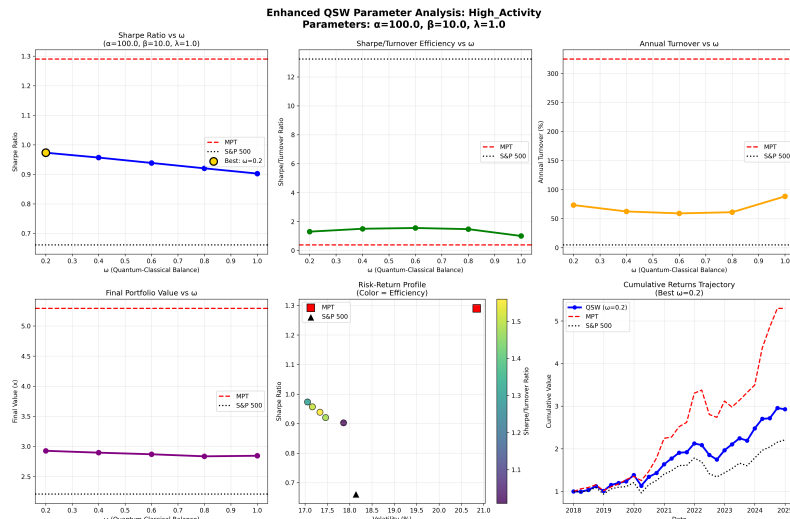


**Fig. 25: 2Y\_High\_Activity** ( $\alpha = 100$ ,  $\beta = 10$ ,  $\lambda = 1$ ). Turnover peaks at 90% (still one-sixth of MPT) with a Sharpe of 0.99 at  $\omega = 0.2$ .